Lehigh University
Lehigh Preserve

Theses and Dissertations

1990

Comparison of the BICEPS and SUPREM simulators with analytical characterization of boron doped silicon epitaxy for a range of growth temperatures

Linda D. Snyder
Lehigh University

Follow this and additional works at: https://preserve.lehigh.edu/etd

Part of the Electrical and Computer Engineering Commons

Recommended Citation
Snyder, Linda D., "Comparison of the BICEPS and SUPREM simulators with analytical characterization of boron doped silicon epitaxy for a range of growth temperatures" (1990). *Theses and Dissertations*. 5318.
https://preserve.lehigh.edu/etd/5318

This Thesis is brought to you for free and open access by Lehigh Preserve. It has been accepted for inclusion in Theses and Dissertations by an authorized administrator of Lehigh Preserve. For more information, please contact preserve@lehigh.edu.

COMPARISON OF THE BICEPS AND SUPREM SIMULATORS WITH ANALYTICAL CHARACTERIZATION OF BORON DOPED SILICON EPITAXY FOR A RANGE OF GROWTH TEMPERATURES

by

Linda D. Snyder

A Thesis

Presented to the Graduate Committee

of Lehigh University

in Candidacy for the Degree of

Master of Science

in

Electrical Engineering

Lehigh University

1989

This thesis is accepted and approved in partial fulfillment of the requirements for the degree of Master of Science in Electrical Engineering.

Sept 18 1989

(date)

Professor in Charge

Chairman of Department

ACKNOWLEDGEMENTS

The author would like to express her appreciation to her advisors R. Jaccodine, at Lehigh University, and P. Langer, at AT&T Bell Laboratories, for their guidance and support. In addition, she would like to thank: C. Paulnack and S. DiDiminico for their help with the epi reactor; C. Clark for electrical measurements; F. Stevie and P. Kahora for their SIMS work; and S.C. Vitkavage, F.G. Herring, and F. Stevie for reviewing this thesis. With special thanks to Susan Vitkavage, who, in addition to reviewing, was never too busy for discussions, guidance, incentive and support.

Most importantly, the author wishes to express her gratitude to her friends and family, all of whom never gave up on her or allowed her to give up on herself.

CONTENTS

1. ABSTRACT 1

2. BACKGROUND 2

2.1 EPITAXY OF SILICON 2

2.2 BICEPS AND SUPREM SIMULATION TOOLS FOR EPI 5

2.3 DESCRIPTION OF MEASUREMENT TECHNIQUES 8

3. EXPERIMENTAL 12

3.1 DESCRIPTION OF EPI EQUIPMENT AND PROCESSING 12

3.2 THICKNESS MEASUREMENTS 13

3.3 SPECIFICS OF SIMULATION RUNS 13

4. RESULTS 15

4.1 ELECTRICAL CONCENTRATION MEASUREMENTS 15

4.2 CONCENTRATION PROFILES 16

5. SUMMARY AND CONCLUSIONS 26

REFERENCES 63

APPENDIX A 65

LIST OF TABLES

TABLE 1. Program diffusivity parameters 28

TABLE 2. Program for epitaxial growth 29

TABLE 3. Microprocessor output definitions 30

TABLE 4. Summary of epitaxy runs 31

TABLE 5. Electrical and chemical concentration results 32

TABLE 6. SUPREM simulation out-diffusion effects 33

TABLE 7. Carrier concentrations 34

TABLE 8. Neutral and positive vacancy state contributions (μ^2/min.) 35

TABLE 9. Empirical and calculated diffusivities 36

LIST OF FIGURES

Figure 1. Impurity distribution in epitaxial growth 37

Figure 2. Four-point probe measurement 38

Figure 3. Spreading resistance technique 39

Figure 4. Schematic of SIMS technique 40

Figure 5. SIMS sample area 41

Figure 6. Epi processing sequence 42

Figure 7. SIMS 1050° C sample analyses with and without prior calibration 43

Figure 8. Simulator variation with concentration input and output request 44

Figure 9. Doping profiles for 1200° C epi 45

Figure 10. Doping profiles for 1150° C epi 46

Figure 11. Doping profiles for 1100° C epi 47

Figure 12. Doping profiles for 1050° C epi 48

Figure 13. Doping profiles for 1000° C epi 49

Figure 14. Doping profiles for 950° C epi 50

Figure 15. Simulator out-diffusion comparison 51

Figure 16. SUPREM out-diffusion effect as a function of temperature 52

Figure 17. Simulator profile shift at defined 50% interface for 1200 and 1150° C 53

Figure 18. Simulator profile shift at defined 50% interface for 1100 and 1050° C 54

Figure 19. Simulator profile shift at defined 50% interface for 1000 and 950° C 55

Figure 20. 1200 ° C SUPREM simulation using Fair model parameters, effective diffusivity with Fair parameters (Fair-X), and default SUPREM parameters 56

Figure 21. 1100 °C SUPREM simulation using Fair model parameters, effective diffusivity with Fair parameters (Fair-X), and default SUPREM parameters 57

Figure 22. 1000 °C SUPREM simulation using Fair model parameters, effective diffusivity with Fair parameters (Fair-X), and default SUPREM parameters 58

Figure 23. Empirical profiles for 1200° C epi run 59

Figure 24. Empirical profiles for 1100° C epi run 60

Figure 25. Empirical profiles for 1000° C epi run 61

1. ABSTRACT

A number of computer simulations have been developed to model the effects of Integrated Circuit (IC) processing on the dopant concentration profiles of semiconductor devices. BICEPS (Bell Integrated Circuit Engineering Process Simulator) and SUPREM (Stanford University PRocess Engineering Models) are two of the more well-known process simulators. The purpose of this work is to explore the accuracy of these simulators for epitaxial processing across a range of temperatures.

The subject of this research was a ten micron p-type epitaxial layer on a heavily doped p-type substrate. The layer was grown in an atmospheric pressure reactor using trichlorosilane as the silicon source and diborane as the dopant gas. The epitaxy processing temperature was varied from 950 to 1200°C in increments of 50°C. Electrically active dopant concentration measurements obtained using the C-V and four-point probe techniques, were used as input to the simulators, and the results of the two simulators were compared with the physical dopant profiles determined using SIMS (Secondary Ion Mass Spectrometry) analysis.

This work showed that boron diffusion during epitaxial growth, on a highly doped substrate, can be simulated reasonably well by use of the simulator programs in the temperature range from 1050 to 1100°C. Outside this range, further work needs to be done.

2. BACKGROUND

2.1 EPITAXY OF SILICON

Epitaxy (epi) of silicon is the growth of single crystal silicon on silicion substrate wafers. Using this deposition process, a multi-layer structure of a lightly doped epitaxial layer and heavily doped substrate can be obtained to enhance the electrical performance of fabricated devices.

Epitaxial processing has developed rather gradually, in comparison with some other Si-LSI (Silicon - Large Scale Integration) industry processes. In the Chemical Vapor Deposition (CVD) epi technology, the basic concept of the deposition process has not been modified since the beginning of the technology. [1]

Epi processing is done across a range of temperatures (500 to 1250°C) and pressures (from atmospheric pressure to $<1\times10^{-8}$ torr), with varying deposition rates (0.001 to 5μm/min). CVD is the most common epi process, which uses gas phase chemical reactions to deposit the desired film on the Si surface. In general, one of the following four (or a combination of these) gases is used as the silicon source: silane (SiH_4), dichlorosilane (SiH_2Cl_2), trichlorosilane ($SiHCl_3$), or silicon tetrachloride ($SiCl_4$). The electrical conductivity of the epitaxial layer is controlled by the amount of dopant gas added. Typically, hydrides of the impurity atoms, arsenic, phosphorous, and boron are used as the dopant gas, namely arsine (AsH_3), phosphine (PH_3), and diborane (B_2H_6), respectively. [2]

The final dopant concentration profile of the epi-substrate structure depends on both the initial substrate doping and the impurities introduced during the epi growth, as illustrated in Figure 1. [3] C_S is the initial substrate doping concentration, C_1 is the doping profile due to

the solid-state diffusion of dopant impurity from the substrate, and C_2 is the profile resulting from the external doping during the epi growth. The interface between the substrate and the epi is located at x=0, and $x=x_f\equiv Vt$ is the epi film surface, where V is the film growth rate and t is the time.

The distribution $C_1(x,t)$ can be obtained by solving the diffusion equation,

$$\frac{\partial C_1}{\partial t}=D\frac{\partial^2 C_1}{\partial x^2}\quad -\infty<x<x_f,\ t>0 \tag{1}$$

where D is the diffusivity of the dopant atoms. Initially, the substrate concentration is uniform,

$$C_1(x,0)=C_S. \tag{2}$$

Additionally, the concentration deep within the substrate will not be affected by the epi process:

$$C_1(-\infty,t)=C_S. \tag{3}$$

The final boundary condition assumes that the material diffusing to the surface of the epi film either escapes into the gaseous ambient at some rate h, where h is the gas-phase mass-transfer coefficient in terms of concentration in the solid, or is incorporated into the film at the growth rate V. This condition is expressed as:

$$-D\frac{\partial C_1}{\partial x}=(h+V)C_1\quad \text{at}\ \ x=x_f\equiv Vt. \tag{4}$$

A rigorous derivation of this condition can be found in reference [3] .

The solution which satisfies the diffusion equation with these conditions is

$$C_1(x,t)/C_S = \frac{1}{2}\text{erfc}[x/2(Dt)^{\frac{1}{2}}] - [(h+V)/2h]\times\exp[(V/D)(Vt-x)]\text{erfc}[(2Vt-x)/2(Dt)^{\frac{1}{2}}]$$
$$+[(V+2h)/2h]\exp[[(V+h)/D][(V+h)t-x]]\times\text{erfc}[[2(V+h)t-x]/2(Dt)^{\frac{1}{2}}]. \quad (5)$$

If the growth rate is high enough such that $Vt/(Dt)^{\frac{1}{2}} \gg 1$ then the impurities are not diffusing to the surface quickly enough to escape. So, regardless of the value of h, the solution reduces to a simple complementary error function

$$C_1(x,t)/C_S \approx \frac{1}{2}\text{erfc}[x/2(Dt)^{\frac{1}{2}}]. \quad (6)$$

The externally introduced dopant is also described by the diffusion equation, but subject to the following initial condition:

$$C_2(x,0) = 0. \quad (7)$$

Deep in the substrate, the external doping impurity vanishes:

$$C_2(-\infty,t) = 0, \quad (8)$$

and, the concentration at the epi film surface is a constant C_f, which is determined by the impurity concentration in the gas:

$$C_2(x_f,t) = C_f. \quad (9)$$

The solution to this problem is

$$C_2(x,t)/C_f=\frac{1}{2}\,1+\mathrm{erf}[x/2(Dt)^{\frac{1}{2}}]+\exp[(V/D)(Vt-x)]\mathrm{erfc}[(2Vt-x)/2(Dt)^{\frac{1}{2}}]. \qquad (10)$$

If $Vt \gg (Dt)^{\frac{1}{2}}$ then the second term can be neglected and this equation can also be reduced to a complementary error function distribution. And, in the epi film, for distances $x>2(Dt)^{\frac{1}{2}}$ from the substrate-epi interface the concentration is $\approx C_f$.

The net impurity distribution $C(x,t)$ is the sum of the substrate and the epi film contributions

$$C(x,t)=C_1(x,t)+C_2(x,t) \qquad (11)$$

for impurities of the same type.

In the range where $Vt \approx (Dt)^{\frac{1}{2}}$, or if $D \neq$constant, or arbitrary initial conditions are considered, the problem does not lend itself to analytical solutions. Therefore numerical solutions have been developed to solve these problems. Two programs which perform such numerical solutions are considered below.

2.2 BICEPS AND SUPREM SIMULATION TOOLS FOR EPI

BICEPS (Bell Integrated Circuit Engineering Process Simulator) and SUPREM (Stanford University PRocess Engineering Models) are computer programs which calculate doping profiles of devices in semiconductor processing. These simulators model ion implantation, predeposition, drive-in under inert or oxidizing conditions, epitaxial growth, deposition, and etch steps. [4] [5] The commands and input requirements for each program are very similar, as evidenced by the sample input files for each simulator which are included as Appendix A.

The simulators use finite difference methods to solve the nonlinear diffusion equations, as outlined above in section 2.1, for each impurity present subject to the boundary conditions described.

Of importance for this work is the program modeling of the diffusivity of boron at the bake and growth temperatures. The diffusivity in both programs is modeled after work by R.B. Fair, which suggests that the effective diffusion coefficient should be the sum of several diffusivities, each accounting for impurity interactions with different charge states of lattice vacancies. [6] Thus, the general form for the diffusion coefficient is

$$D_i = D_i^x + D_i^- f + D_i^+ / f + D_i^= f^2 + \cdots \quad (12)$$

$$f = \frac{n}{n_i} \quad (13)$$

where D_i^x , D_i^- , D_i^+ , $D_i^=$ are the intrinsic diffusivities of various vacancy states, n is the electron concentration, a function of all C_i, and n_i is the intrinsic electron concentration at the process temperature.

As an acceptor, boron is negatively charged in the silicon lattice, and it diffuses primarily with positive (D^+) and neutral (D^x) vacancies. Thus, the diffusivity of boron is largely determined by the following contributions:

$$D_i = D_i^x + D_i^+ \left[\frac{n_i}{n} \right] \quad (14)$$

The vacancy state diffusivities can be described by equations of the form:

$$D_i^* = D_{i0}^* e^{\frac{-Q_i^*}{kT}} \tag{15}$$

where D_{i0}^* is a prefactor and Q_i^* is the activation energy. The values for these coefficients used by BICEPS and SUPREM are presented in Table 1. Also presented in this table are the coefficients provided by Fair. [7] The differences in these coefficients and their effects on the simulation profiles will be discussed in results.

The electron concentration, n, can be approximated by use of the mass action law and charge neutrality [8]

$$n = \frac{1}{2}[C_{net} + (C_{net}^2 + 4n_i^2)^{0.5}] \tag{16}$$

$$C_{net} = -\sum_{i=1}^{i=n} Z_i N_i \tag{17}$$

where Z_i is the charge state of the ith impurity (=1 for acceptors, =-1 for donors) and N_i is the electrically active concentration of the ith impurity. The intrinsic electron concentration, n_i, is calculated using the Morin-Maita relation [9]

$$n_i = 3.87\times10^{16} T^{1.5} e^{-\frac{E_g}{2kT}} \tag{18}$$

$$E_g = 1.21 - 7.1\times10^{-10} n_i^{0.5} T^{-0.5} \tag{19}$$

where E_g is the energy band gap of silicon, k is the Boltzmann's constant, and T is the temperature in degrees Kelvin.

The details of the simulators' application of the diffusivity model presented above will be explored for each simulator in the results section.

2.3 DESCRIPTION OF MEASUREMENT TECHNIQUES

2.3.1 C-V MEASUREMENT

C-V measurements were used to determine the doping level in the epitaxial layer. A mercury contact is used to form a Schottky barrier diode, which is reverse-biased. The doping level is determined from the relationships:

$$N(x) = C^3 \left[\frac{dC}{dV}\right] qA^2\varepsilon_s \qquad (20)$$

$$x = \varepsilon_s A/C \qquad (21)$$

where C is capacitance, V is voltage, q is charge, A is the diode area, ε_s is the dielectric permittivity of silicon, N is the doping density, and x is the depth. [10]

2.3.2 FOUR-POINT PROBE MEASUREMENT

The substrate doping level was determined using the four-point probe method on the back side of the wafers. In this technique, which is illustrated in Figure 2, [11] four probes are placed on the semiconductor surface, and current is passed through the two outermost probes. The voltage across the two inner probes is monitored. This eliminates any problems due to the probe-to-semiconductor contact resistances. The spreading of the current, as shown in the top view of Figure 2, must be taken into account. This has been done, and for layers with large lateral dimensions and small x_j compared to the probe spacing, the voltage drop V and current I have been shown to be related to the average resistivity $\bar{\rho}$ of the diffused layer by the equation:

$$\bar{\rho} = \frac{\pi}{\ln 2}\frac{V}{I}x_j = 4.532\frac{V}{I}x_j \tag{22}$$

Substituting the wafer thickness for x_j allows calculation of the substrate resistivity, and, hence, the dopant concentration. Correction factors are applied if either x_j or the wafer thickness are comparable to the probe spacing. The resistivity is then converted to concentration. [12]

2.3.3 SPREADING RESISTANCE MEASUREMENTS

The two-point probe spreading resistance technique was used to obtain the electrically active dopant profiles. For this measurement, the sample is mounted on an angle block and beveled or polished to a known angle, as shown in Figure 3. The probes are stepped down the incline as the spreading resistance is measured. The total spreading resistance is given by

$$R_{sr} = \frac{\rho}{2a} \tag{23}$$

where R_{sr} is the spreading resistance, ρ is the average resistivity near the probe points, and a is the probe radius.

This resistance is then converted to the electrically active ion concentration using a calibration curve, which is dependent upon the wearing of the probe points. Because the measurements are sensitive to the surface conditions of the sample and the condition of the probe points, spreading resistance measurements are generally used for concentration profiling, rather than the absolute concentration value determination.

2.3.4 SIMS

The SIMS (Secondary Ion Mass Spectrometry) technique was used to obtain the atomic

profile of the samples. Figure 4 is a schematic representation of the SIMS instrumentation. SIMS utilizes an ion beam to sputter material from the sample. The ionic component of the sputtered material is mass analyzed and counted by the detector. [13]

The SIMS method provides a means of profiling the concentration of trace constituents with depth resolution as low as 50A. High current density sputtering, with its accompanying high surface removal rates, is required for obtaining elemental depth profiles and trace element analyses.

The depth profile is obtained by monitoring the secondary ion signal as a function of time. Since the samples of interest in this case consist of a homogeneously distributed trace element in a single crystal matrix, the absolute ion intensity is directly proportional to the concentration at a given depth.

The detection sensitivity for the element in a given matrix is dependent on the characteristics of the element itself, the chemical composition of the matrix, the primary ion beam species, and instrument dependent and controllable parameters.

The positive cesium ion beam is generally useful for obtaining high negative ion yields from a target, while O_2^+ primary ion beams are usually used for generating high positive ion yields from electropositive species. However, F. Stevie, et al. [14] have shown a correlation between secondary ion yield changes and changes in the surface topography using an O_2^+ primary beam for analysis of Si at depths greater than about 3μm. Hence, the boron profiles in this work were produced using a Cs^+ primary beam. The boron detection limit under these conditions is $\approx 4\times10^{15}\,cm^{-3}$ on the CAMECA IMS-3f which was used for the analysis.

Quantitation is accomplished by the use of standards to determine relative elemental

sensitivities. Generally, with robust standards and sample homogeneity, accuracies of 10% can be obtained. A profile was made on a boron implant standard to quantify the results.

During the SIMS depth analysis, the primary ion beam, of diameter ≈80μm, is rastered to produce crater of ≈220×220μm. The secondary ion analyzed area is a circle with ≈60μm diameter taken from the center of this crater, as shown in Figure 5.

3. EXPERIMENTAL

3.1 DESCRIPTION OF EPI EQUIPMENT AND PROCESSING

An Applied Materials model 7800 RP radiantly heated barrel reactor was used to grow the epi layer. Three wafers per run were loaded onto a six(6)-sided graphite susceptor, one wafer on every other face in the middle row. The reactor is microprocessor controlled, and the program is set up by the on/off settings of various control switches.

The program used for this work is detailed in Table 2. Table 3 contains an explanation of the control switches for the equipment.

The processing sequence is depicted in Figure 6. This graph shows the thermal treatment of the wafers as a function of time. In general, an HCl etch is performed prior to epitaxial growth to remove particles and surface damage, but an H_2 bake was substituted in this work so that no anomolous impurity redistribution due to etch effects would be introduced.

Six runs were made with a temperature variation from 950 to 1200°C. The epi growth time was adjusted following each run dependent on the previous run in an attempt to grow a nominal ten micron layer.

The silicon source gas is trichlorosilane, and diborane is the dopant gas. Before processing, the 125mm diameter, <100> oriented wafers were back-sealed with an oxide-nitride layer, so that auto-doping effects would be negligible. Otherwise, at the high temperatures used for epi growth, the boron in the substrate could diffuse out from the backside of the wafer and alter the concentration by incorporation into the growing epi layer.

3.2 THICKNESS MEASUREMENTS

The thickness measurements were done on a Qualimatic automated measurement tool. This instrument is a Fourier transform interferometer, which determines the interface by the difference in the index of refraction for the substrate and the epi. The real part of the refractive index is the same for both layers, but the imaginary part includes the doping level difference.

No claims can be made as to the accuracy of this interface depth measurement instrument, since the definition of the interface is not standard. Instead, the inter-lab reproducibility for the instrument is reported as ±2½% of the film thickness. This is the 3σ for the measurement reproducibility.

3.3 SPECIFICS OF SIMULATION RUNS

The epitaxial growth in this work was modeled as follows. In both cases, the substrate is initialized as <100> silicon with a boron concentration equal to that measured using the four-point probe method.

This is followed by a ramp up and stabilization at the temperature of interest. The ramp up time is based on a temperature ramp rate of 70° C/min., and both the ramp up and the stabilization are done in an inert ambient. The actual inert gas used is H_2, however, nitrogen is used to simulate the inert, or non-oxidizing, ambient in SUPREM.

The epi layer is grown at a concentration which was determined experimentally. The samples were C-V tested for the electrically active boron concentration, and this value was used in the simulations. The growth rates were determined from the actual growth time and the measured epi thickness.

At the end of the deposition cycles, the silicon source and dopant gases are purged for two minutes at the growth temperature. And, finally, the temperature is ramped down to 850°C, where the power to the lamps is turned completely off.

As examples, the input files for the 1150°C BICEPS and SUPREM simulations are included in Appendix A.

4. RESULTS

Table 4 lists the epi runs with the run temperature and deposition time, along with the average epi thickness per run and the calculated deposition rate.

4.1 ELECTRICAL CONCENTRATION MEASUREMENTS

All three samples in each run were measured using the spreading resistance technique. The results were compared and the wafer-to-wafer consistency within a run was quite good. The shapes of the measured doping profiles are very similar, and the epi and substrate concentrations from wafer-to-wafer agree to within ≤25%. In addition, the wafer-to-wafer interface depth agreement, assuming the interface is defined as the point of 50% of the substrate concentration, is good to ≤5% in all but the 1200°C run, where the variation is ≈13%.

The results of the C-V and four-point probe measurements are summarized in table 5. The C-V measurement for the 950°C sample is absent, because the surface was either polycrystalline or simply too rough to make a good diode with the mercury contact. If a polycrystalline film was grown at 950°C, the effects of the crystal boundaries could complicate the problem enormously, therefore, this run will not be detailed in the following discussions. In addition, the values of the epi and substrate concentrations, determined from the spreading resistance measurements and SIMS analyses, are included in this table for comparison.

The validity of the epi layer concentrations determined by SIMS is in question, since the measured boron concentrations are near the detection limit of the instrument. The low initial boron concentration gives rise to yet another problem. The mass analyzer of the SIMS must

be tuned for the mass peaks of interest, in this case, B^{10} and B^{11}, which are relatively narrow peaks. Even a slight variation from the peak could cause a significant loss in the number of ions detected. Since the boron is undetectable at the start of the profile, the tuning must be done by predetermined values obtained from a boron sample. The magnet in the mass analyzer can experience some drift in these mass numbers, so the calibration sample must be run immediately prior to the actual sample measurement. Three of the samples needed to be rerun for SIMS profiles; the 950, 1050, and 1150°C runs. The substrate concentration values determined from the rerun samples are included in Table 5. Figure 7 shows the SIMS data for the 1050°C epi run, both with and without prior calibration runs.

Even when calibration samples are run immediately prior to the sample of interest, some loss of signal can occur due to the drift in the mass analyzer. As a result of these findings, the SIMS staff is exploring alternative methods for analyzing samples where the element of interest is undetectable at the start of the analysis.

4.2 CONCENTRATION PROFILES

In order to determine the variability of the simulated profiles for differing input concentrations, the substrate and epi concentrations for the simulation runs were varied between the chemical concentrations obtained from SIMS and the values obtained from the electrical measurements, using the SUPREM program. The shape of the interface concentration curve did not change, as evidenced by curves 1 and 2 of Figure 8. Note that the curve using the electrical values as input and requesting the active profile output (1-elec.,active) does not differ significantly from the curve using the chemical, or SIMS, values as input and again requesting an active profile (2-chem.,active).

In addition, with the SUPREM program, active or chemical profiles can be requested as output. Simulations were run asking for both types of profile for comparison. No difference was observed, as the comparison of the active profile (2-chem.,active) and the chemical profile (3-chem.,chem.) in Figure 8 demonstrates.

The concentration profiles for the six temperatures are shown in Figures 9 through 14. These simulations were run using the four-point probe and C-V electrical measurements as input for the substrate and epi concentrations, respectively. The figures include the simulation profiles, and the SIMS and spreading resistance measurement (SRM) profiles. The full epi layer and a close-up of the interface area are shown.

The BICEPS and SUPREM simulations appear to track very closely. However, SUPREM accounts for the out-diffusion of impurities at the epi film surface, which appears as a small tail near x=0 on all of the temperature profiles. The amount of out-diffusion increases with increasing temperature, as expected. During the epi growth, the BICEPS program includes a 0.01µm oxide which would inhibit any escape of impurities. Even adding an etch step to the simulation, prior to the growth, did not keep this oxide from being included.

In addition, there is a slight deviation of the simulators at the substrate-epi interface, which increases with increasing temperature. BICEPS does not consider out-diffusion of the impurity from the substrate surface during the H_2 bake prior to epi growth, which could account for the difference. Evidence for this effect is shown in Figure 15, which shows the SUPREM 1200°C vs. the BICEPS 1200°C simulation after the bake and before the epi growth. The BICEPS profile stays flat (uniform concentration) while near the surface, the SUPREM profile curves downward (loss of impurity at the surface). The SUPREM

simulations in Figure 16 show the substrate surface after the H_2 bake for three of the subject temperatures. Table 6 summarizes the amount of out-diffusion occuring at each process temperature. This table lists the four-point probe substrate concentration, C_S, the substrate surface concentration which was reduced due to out-diffusion, C_{od}, and the % difference in the surface concentration ($\frac{C_S - C_{od}}{C_S} \times 100$). The bake times are also included in this table, since they were not equal. The times to ramp up to and stabilize at the process temperature were 15 min. for all runs, and since the ramp rate was 70° C/min. in all cases, it took less time to reach the lower temperatures. So, at the lower temperatures, the wafers received a longer bake. The out-diffusion effect is more pronounced at higher temperatures, even with the shorter bake times.

The measured interface depth is included on the close-up profiles in Figures 9 through 14. The SIMS profiles are skewed from these values, suggesting some error in the Qualimatic thickness measurements. This error would also be incorporated in the simulations, since the measured epi thickness values were used to calculate the growth rates, which were used as input to the simulators.

Fortunately, the important aspect of these profiles, for studying diffusivity, is their shape, rather than the absolute values of either the depth or the concentrations. Thus, the curves can still be analyzed once this error is determined and removed. For simplicity, the SUPREM simulations are used in the following treatment of results, since they included the out-diffusion effects and were, therefore, considered more realistic.

A useful benchmark, employed by epi processors and SIMS analysts alike, is the 50% interface. In other words, the point at which the concentration is 50% of the substrate

concentration is taken as the interface between the layers. This 50% interface construct is used to shift the simulator profiles to the SIMS profiles, so that meaningful comparisons can be made.

The adjusted SUPREM profiles are shown in Figures 17, 18, and 19. The adjusted SUPREM simulation for the 1050 and 1100°C run are fairly good. However, even with the adjustment for depth measurement error, the simulator is not adequately profiling the SIMS data for the other temperatures considered. Thus the diffusivity model and the coefficients employed by the simulators warrant further discussion.

Table 7 lists the values for the intrinsic (n_i) and free (n) carrier concentrations. The values for the intrinsic carrier concentration for the two simulators tracked very closely. The values of n_i used in BICEPS were output by the program in the standard BICEPS output files for the simulation run at each temperature. The SUPREM values of n_i were calculated from a prefactor, ni.0, and activation energy, ni.e, which were requested by a PRINT statement in the program. The output of this statement contained the values which were used in the following equation:

$$n_i = ni.0\ T^{1.5}\ e^{-ni.e/kT} \qquad (24)$$

Substituting n_i into equation 16, and using $N_i=C_S$ (in equation 17), where C_S is the measured four-point probe concentration used as input to the simulator, one can calculate the free carrier concentration, n.

As discussed in section 2.2, the diffusivity of boron can be calculated from

$$D = D^x + D^+ \left[\frac{n_i}{n} \right]. \tag{25}$$

The ratio $\frac{n_i}{n}$ affects the overall contribution of the positive vacancy states (D^+) to the total boron diffusivity (D), according to the model. From the table, the temperature dependence of this ratio is obvious. As the temperature increases, the quantity of free carriers increases at a higher rate than the intrinsic carriers, and the relative effect of the positive vacancy state diffusivity decreases.

Table 8 lists the diffusivity contributions for the neutral and positive vacancy states for the models and the original Fair model. The actual contribution of each of the vacancy states is not consistent across the simulators or the Fair model. Excluding the additional weighting effect of the carrier concentration ratio ($\frac{n_i}{n}$), the Fair model weights the positive vacancy factor more heavily than the neutral vacancy factor, as does the BICEPS simulator. The SUPREM program, on the other hand, gives more weighting to the neutral factor. The positive factor in the Fair model is 19.7 times larger than the neutral. In BICEPS, the positive factor is 3 times larger. Finally, in SUPREM, the neutral factor is larger by a factor of 1.2. Despite the differences in the application of the diffusivity model, the curves produced by BICEPS and SUPREM are similar. The agreement of the Fair model and SUPREM is discussed in more detail below.

The SUPREM documentation [5] quotes the values of the parameters from the original Fair model, however, the actual program used appears to have been altered, perhaps to include more recent data. The difference between the SUPREM simulation using the default parameters and the SUPREM simulation using the Fair parameters as input is shown in

Figures 20 through 22 for 1200, 1100, and 1000°C. The default simulations display slightly larger effective diffusivities than the simulations with Fair's parameters, at all temperatures. This is evidenced by the smearing, or increased slope, of the interface. The effect is more noticable at 1200 and 1000°C.

The third curve in each of the figures, which is marked "Fair-X," represents the simulation run using an "effective" diffusivity, which is concentration independent and was calculated using the Fair coefficients. The neutral vacancy state of the Fair model does not change with concentration, as the contribution due to the positive vacancy state does. A concentration-independent diffusivity, in terms of the vacancy state model, is a diffusivity based solely on the neutral state. The effective diffusivity, then, is calculated by adding the contributions from each of the states (with the ratio $\frac{n_i}{n} = 1$), and assigning the total to the neutral state contribution, and the coefficients for the positive contribution are set to zero.

$$D_{eff} = D^x \tag{26}$$

This was accomplished with the following input line in SUPREM:

```
BORON     SILICON DIX.0=4.542E9 DIX.E=3.46 DIP.0=0 DIP.E=0
```

It is clear from Figure 18 that ignoring the concentration dependence does not have a significant effect on the output of the simulator at 1100°C. The diffusivity appears to have little or no concentration-dependence at this temperature. In addition, at 1200 and 1000°C, where the Fair and Fair-X profiles do differ noticably, the Fair-X curve actually tracks the SIMS data more closely.

It has been noted by Fair [7] that few sources of reliable, unambiguously extracted diffusivity data exist. Antoniadis et al. [15] attribute the abundance of conflicting values of boron diffusion coefficients to the effects of extrinsic conditions. The terms intrinsic and extrinsic in the following discussion refer to the condition of the silicon at the process temperature. The silicon is intrinsic when the doping level is sufficiently low that it does not affect the impurity's diffusivity. In the extrinsic regime, on the other hand, the diffusivity is concentration dependent. Boron diffusivity is independent of impurity concentration provided that the boron concentration is lower than that of intrinsic carriers at the process temperature. A comparison of the intrinsic carrier concentrations (n_i) in Table 7 and the substrate concentrations listed in Table 5 shows that the silicon could be considered extrinsic at the lower temperatures. The transition temperature seems to be at or below ≈1050°C. However, the concentration at the epi substrate interface drops off rather quickly. The loss of impurity due to the out-diffusion effect discussed earlier, and summarized in Table 6, results in the silicon reverting to intrinsic conditions as the concentration drops below the intrinsic carrier concentration. Thus, the silicon is effectively intrinsic for the entire epi processing time. At the higher temperatures considered in this work the silicon is safely in the intrinsic range and the diffusivity of the boron can be considered concentration independent. At the lower temperatures, the silicon is intrinsic during the bulk of the processing time.

With the assumption of intrinsic behavior, it follows that the boron diffusivity, for the conditions studied in this work, should reasonably reflect that found in the literature. Three sources of empirical data for boron diffusivity were considered. The SUPREM documentation referred to earlier [5] unpublished work of Lin et al., which will be referred to as work by Lin. The other two sources were work by Antoniadis et al. [15], and the Bell

Laboratories Quick Reference Manual (QRM). [16] Table 9 lists the diffusivity data obtained from these sources. These values are approximate, since they were taken from graphs. The table shows the value obtained from the literature in $cm^2/sec.$, which was converted to $\mu^2/min.$. The empirical values of D are in fairly close agreement at the lowest temperature presented, and they diverge somewhat at the higher temperatures. The values from the Lin and QRM sources were used to run simulations. The value of D^x was calculated so that simulations could be run. The simulations were run using this number with the Fair value for the activation energy, to obtain an effective diffusivity. In other words, only the neutral vacancy contribution was non-zero, as described earlier. Simulation runs were done for the 1200, 1100, and 1000°C epi runs.

In addition, values for effective diffusivities at 1200, 1100, and 1000°C were calculated from the SIMS data. From section 2.1, the interface profile can be approximated as (equation 6):

$$C_1(x,t)/C_S = \frac{1}{2}\text{erfc}[x/2(Dt)^{\frac{1}{2}}]. \quad (27)$$

Or, solving for C_1

$$C_1(x,t) = \frac{C_S}{2}\text{erfc}[x/2(Dt)^{\frac{1}{2}}]. \quad (28)$$

Considering the depths at which the concentration was 50% and 0.5% of the substrate value (i.e. - a drop in concentration of two decades, or 10^{-2}), and replacing the complementary error function with its definition, we obtain

$$\frac{C_S}{2}\times 10^{-2} = \frac{C_S}{2}(1-\mathrm{erf}[\frac{x}{2(Dt)^{\frac{1}{2}}}]), \tag{29}$$

which reduces to

$$\mathrm{erf}[\frac{x}{2(Dt)^{\frac{1}{2}}}] = 0.99 \tag{30}$$

Then, referring to a table of error functions [17]

$$\frac{x}{2(Dt)^{\frac{1}{2}}} = 1.82. \tag{31}$$

Solving for D yields

$$D = \frac{x^2}{13.25\times t} \quad \text{in } \mu^2/\text{min}. \tag{32}$$

Substituting the value $x=\Delta x$, where Δx is the difference in depth from the 50% to the 0.5% concentrations from the SIMS data, the diffusivity can be calculated. These values are included in Table 9.

Figures 23, 24, and 25 show the empirical simulations along with the SIMS profiles, the default SUPREM simulations, and the simulation profiles using the calculated diffusivities, for the temperatures considered. At 1200°C the Lin empirical curve tracks the SIMS profile much better than the default SUPREM simulation. The QRM and calculated curves, on the other hand, overshoot the diffusivity at this temperature. For the 1100°C simulations, there is no significant difference between the Lin empirical data, the QRM data, and the calculated value for diffusivity. All of these effective diffusivities model the SIMS data fairly well.

Again, as above at the higher temperature, the profile using the calculated value overshoots the SIMS profile. At 1000°C the profiles using the empirical data from Lin and the QRM, and the default SUPREM simulation produce very similar profiles, which fall short of the SIMS data. The values for diffusivity from the three sources of data are in fairly good agreement at the lower temperature, but they do not accurately model the SIMS data, as noted. This suggests that either the empirical data is off at the lower temperatures or the silicon is in the extrinsic regime, and an effective diffusivity cannot accurately model the profile. The value calculated from the SIMS profile also overshoots the SIMS curve at this temperature.

5. SUMMARY AND CONCLUSIONS

The BICEPS and SUPREM simulator concentration profile output for boron doped epi growth on <100> silicon has been compared to SIMS data, across the temperature range from 950 to 1200°C. Measurements were also made on the electrically active dopant concentrations using the spreading resistance technique, C-V measurements, and the four-point probe method. Although the simulators were relatively accurate in the midrange of the temperatures considered, the simulators did not emulate the SIMS profiles with any degree of accuracy outside the temperature range from 1050 to 1100°C.

The output from the BICEPS and SUPREM simulators was very similar. However, the SUPREM simulator was more accurate in its handling of the impurity out-diffusion effect both during the pre-epi growth thermal treatment of the wafers and during the epi growth. BICEPS ignored these effects altogether. Thus, the additional simulations discussed were run on SUPREM. The effect of the concentration dependent contribution of the diffusivity, which is proposed by Fair's model and used by both simulators, was also explored.

The simulators and Fair's model were compared and contrasted, and the relative contributions of the positive and neutral vacancy states were discussed. In addition, an effective boron diffusivity, which is concentration independent, was calculated for the Fair model, and simulations were run using this effective diffusivity. These were compared with the model, and no significant difference was found between 1050 and 1150°C.

Empirical data from three literature sources were compared and contrasted. An effective diffusivity was derived from the data and simulation comparisons done. At high temperatures, simulations using the effective diffusivity from the QRM data tracked the SIMS data very well. Below the temperature at which the silicon becomes extrinsic, the

empirical data did no better than the default SUPREM simulation. Values for the effective diffusivity were also calculated from the SIMS curves. The profiles run using these values generally overshot the SIMS curves. As with the above data, the best agreement was at 1100°C.

Boron diffusion during epitaxial growth, on a highly doped substrate, can be simulated reasonably well by use of the simulator programs in the temperature range from 1050 to 1100°C. Outside this range, further work needs to be done.

This work also shed some light on a SIMS measurement weakness. The low impurity concentration of the epitaxial layer of the experimental samples resulted in detection error in the SIMS technique. This problem was investigated by the SIMS staff, and alternative methods for analyzing this type of sample are being explored.

	D_{i0}^{x} (μ^2/min.)	Q_i^x (eV)	D_{i0}^{+} (μ^2/min.)	Q_i^+ (eV)
BICEPS	8.33e8	3.43	2.5e9	3.43
SUPREM	1.68e9	3.40	1.38e9	3.40
Fair model	2.22e8 (0.037cm^2/s)	3.46	4.32e9 (0.72cm^2/s)	3.46

TABLE 1. Program diffusivity parameters

Epi process program*

Time	Function	Output
6.0	High H_2 purge	1,3
5.5	Heat to 850°C (SP 4)	2,3,18
1.0	Stabilize at 850°C	2,3,18
6.0	Heat to bake temperature (SP 2)	2,3,16
2.0	Stabilize at bake temp	2,3,16
3.0	H_2 bake	2,3,16
2.0	H_2 purge	2,3
2.0	Stabilize, purge trichlor, dopant	2,3,8,9,19
5.0	Deposit epi	2,3,8,9,15,19
1.0	Deposit epi	2,3,8,9,15,19
1.0	Deposit epi	2,3,8,9,15,19
1.0	Deposit epi	2,3,8,9,15,19
1.0	Deposit epi	2,3,8,9,15,19
1.0	Deposit epi	2,3,8,9,15,19
2.0	H_2 purge	2,3
3.0	Cool to 850°C	2,3,18
6.0	Heaters off, H_2 purge	3
4.0	N_2 purge End	End

* Shown for 10 minute deposition

TABLE 2. Program for epitaxial growth

Output	Function
1	High purge
2	Heater
3	H_2
4	HCl source
5	HCl etch
6	High HCl etch
7	D_n inject
8	D_p inject
9	SiH_4
10	SiH_2Cl_2
11	$SiCl_4$
12	$SiHCl_3$
13	Aux 1
14	Aux 2
15	Deposit
16	Temp SP (set point) 2
17	Temp SP 3
18	Temp SP 4
19	Main Flow SP 2
20	Main Flow SP 3
21	Main Flow SP 4
22	Main Flow OFF
23	Slow VAC pump
24	High VAC pump
25	Leak check
26	
27	Si ramp
28	Si ramp hold
29	Dope ramp
30	Dope ramp hold
31	Temp ramp
32	Temp ramp hold

TABLE 3. Microprocessor output definitions

Dep. temp. (°C)	Dep. time (min.)	Avg. thick. (μm)	Calculated dep. rate (μm/min.)
1200	10.0	9.82	0.982
1150	10.0	10.11	1.011
1100	10.0	9.84	0.984
1050	10.0	8.60	0.860
1000	15.0	9.21	0.614
950	26.0	12.70	0.488

TABLE 4. Summary of epitaxy runs

	Electrical				Chemical		
Temp (°C)	Epi (C-V)	Substrate (4pt probe)	Epi (SRM)	Substrate (SRM)	Epi (SIMS)	Substrate (SIMS)	Substrate (SIMS-2)
1200	2.4e15	1.4e19	1e16	2e19	4.0e15	1.3e19	------
1150	1.6e15	1.1e19	5e15	2e19	4.0e15	8.0e18	6.5e18
1100	1.2e15	1.3e19	4e15	2e19	3.8e15	1.0e19	------
1050	8.0e14	1.2e19	2e15	2e19	4.1e15	3.0e18	1.0e19
1000	7.1e14	1.2e19	2e15	2e19	2.0e15	1.0e19	------
950	------	1.2e19	2e13	2e19	4.7e15	4.0e18	6.5e18

TABLE 5. Electrical and chemical concentration results

Temperature (°C)	C_S	C_{od}	% difference	Bake time (min.)
1200	1.4e19	3.82e18	72.7	10.0
1150	1.1e19	3.41e18	69.0	10.7
1100	1.3e19	4.90e18	62.3	11.4
1050	1.2e19	5.39e18	55.1	12.1
1000	1.2e19	6.49e18	45.9	12.9
950	1.2e19	7.71e18	35.7	13.6

TABLE 6. SUPREM simulation out-diffusion effects

Temperature (°C)	BICEPS n_i (cm^{-2})	SUPREM n_i (cm^{-2})	SUPREM n (cm^{-2})	n_i/n
1200	2.732e19	2.698e19	2.09e19	1.291
1150	2.138e19	2.123e19	1.64e19	1.295
1100	1.650e19	1.644e19	1.12e19	1.468
1050	1.254e19	1.252e19	9.88e18	1.589
1000	9.367e18	9.347e18	5.11e18	1.829
950	6.866e18	6.833e18	3.09e18	2.211

TABLE 7. Carrier concentrations

Temperature (°C)	BICEPS D_i^x	BICEPS D_i^+	SUPREM D_i^x	SUPREM D_i^+	Fair model D_i^x	Fair model D_i^+
1200	1.55e-3	4.65e-3	3.96e-3	3.25e-3	3.26e-4	6.34e-3
1150	6.00e-4	1.80e-3	1.54e-3	1.27e-3	1.25e-4	2.43e-3
1100	2.17e-4	6.50e-4	5.63e-4	4.62e-4	4.48e-5	8.72e-4
1050	7.25e-5	2.18e-4	1.90e-4	1.56e-4	1.48e-5	2.89e-4
1000	2.22e-5	6.68e-5	5.90e-5	4.84e-5	4.51e-6	8.78e-5
950	6.20e-6	1.86e-5	1.66e-5	1.36e-5	1.24e-6	2.42e-5

TABLE 8. Neutral and positive vacancy state contributions (μ^2/min.)

	QRM	Lin	Antoniadis	Calc.
1200(°C)				
D (cm^2/sec)	2.6e-12	1.8e-12	1.0e-12	
D (μ^2/min)	1.56e-2	1.08e-2	6.0e-3	1.5e-2
D^x (μ^2/min)	1.06e10	7.36e9	4.09e9	1.02e10
1100(°C)				
D (cm^2/sec)	2.4e-13	2.0e-13	1.5e-13	
D (μ^2/min)	1.44e-3	1.2e-3	9.0e-4	1.6e-3
D^x (μ^2/min)	7.14e9	5.95e9	4.46e9	7.93e9
1000(°C)				
D (cm^2/sec)	1.6e-14	1.4e-14	1.2e-14	
D (μ^2/min)	9.6e-5	8.4e-5	7.2e-5	6.4e-4
D^x (μ^2/min)	4.73e9	4.14e9	3.54e9	3.15e10

TABLE 9. Empirical and calculated diffusivities

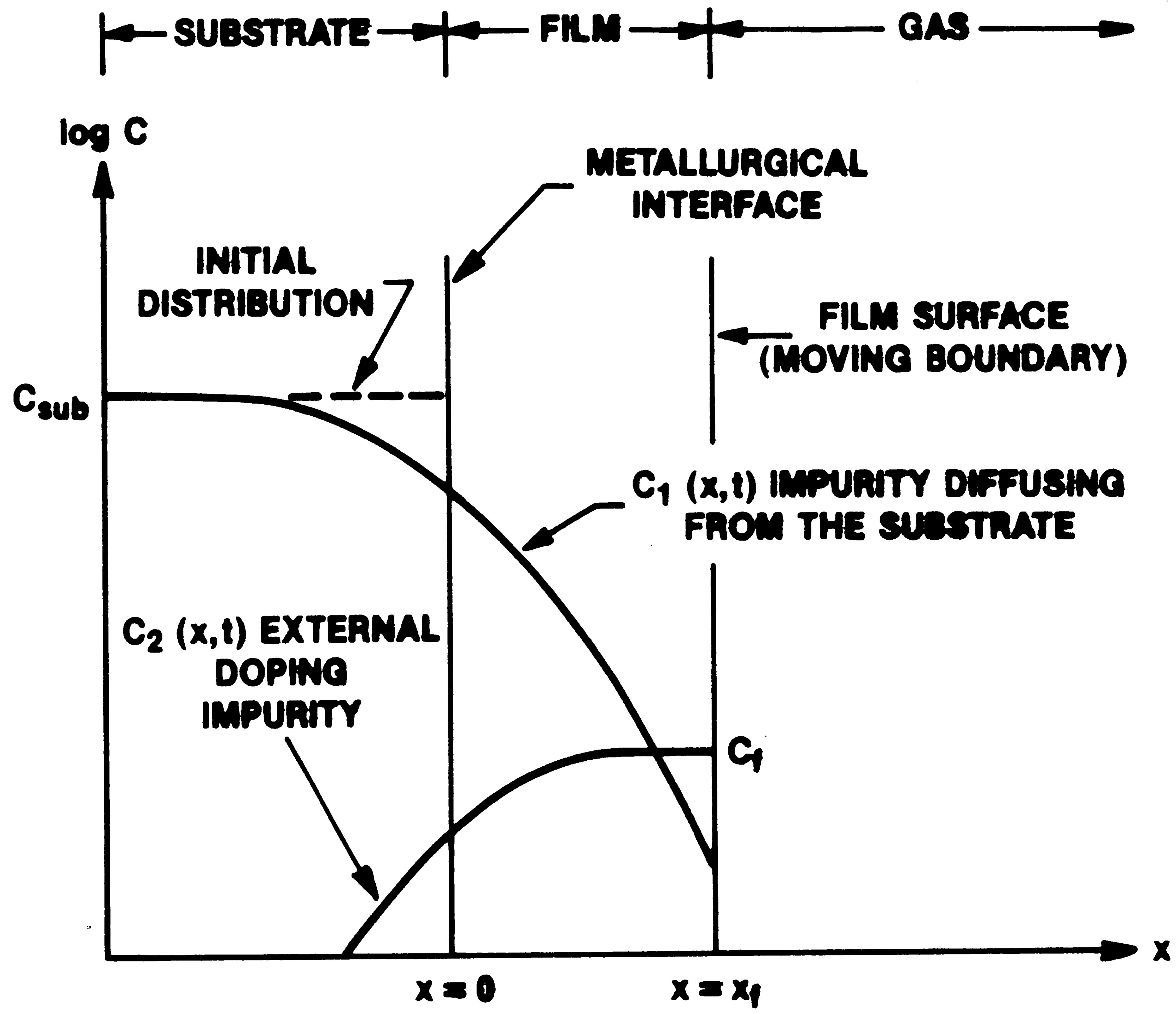

Figure 1. Impurity distribution in epitaxial growth

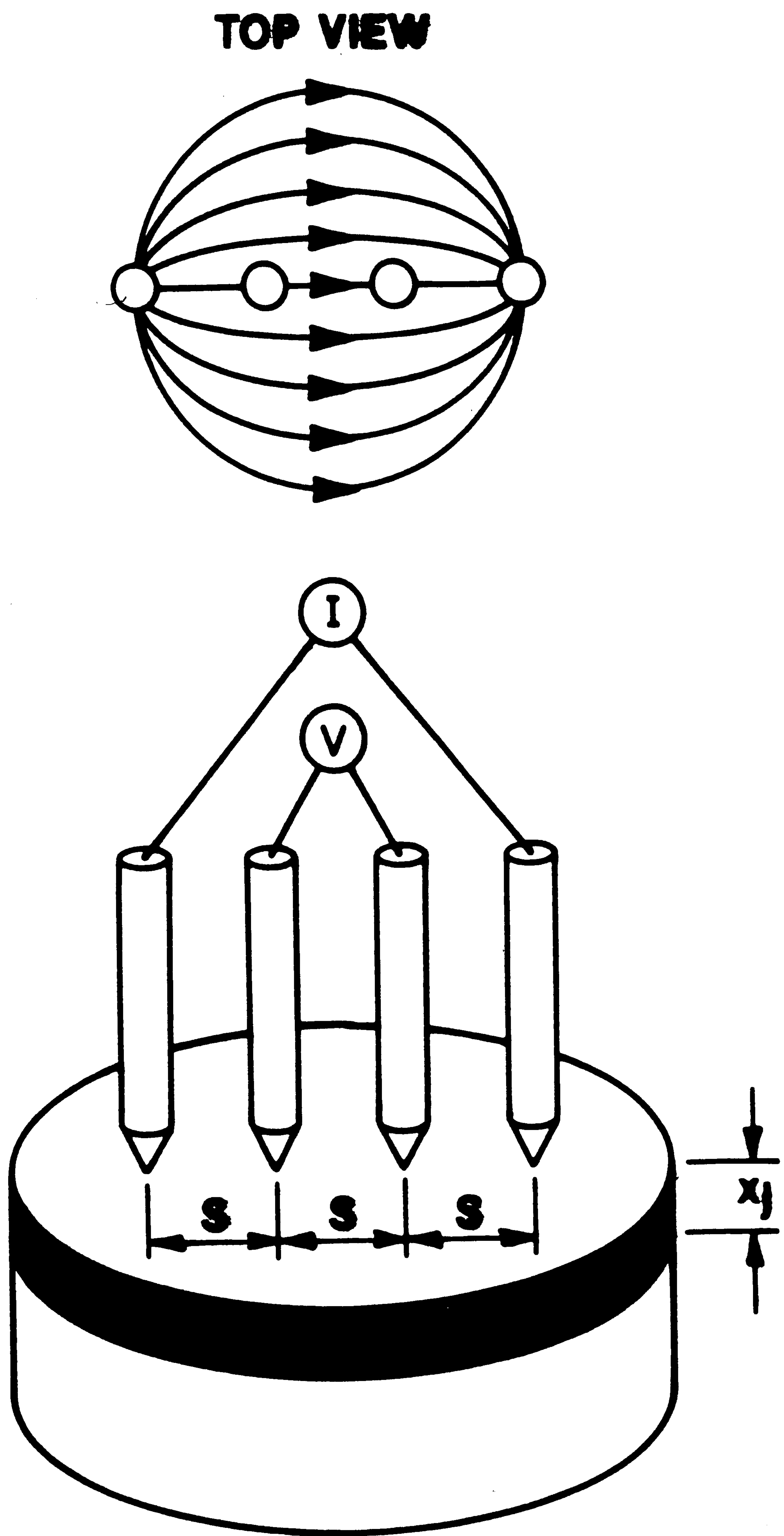

Figure 2. Four-point probe measurement

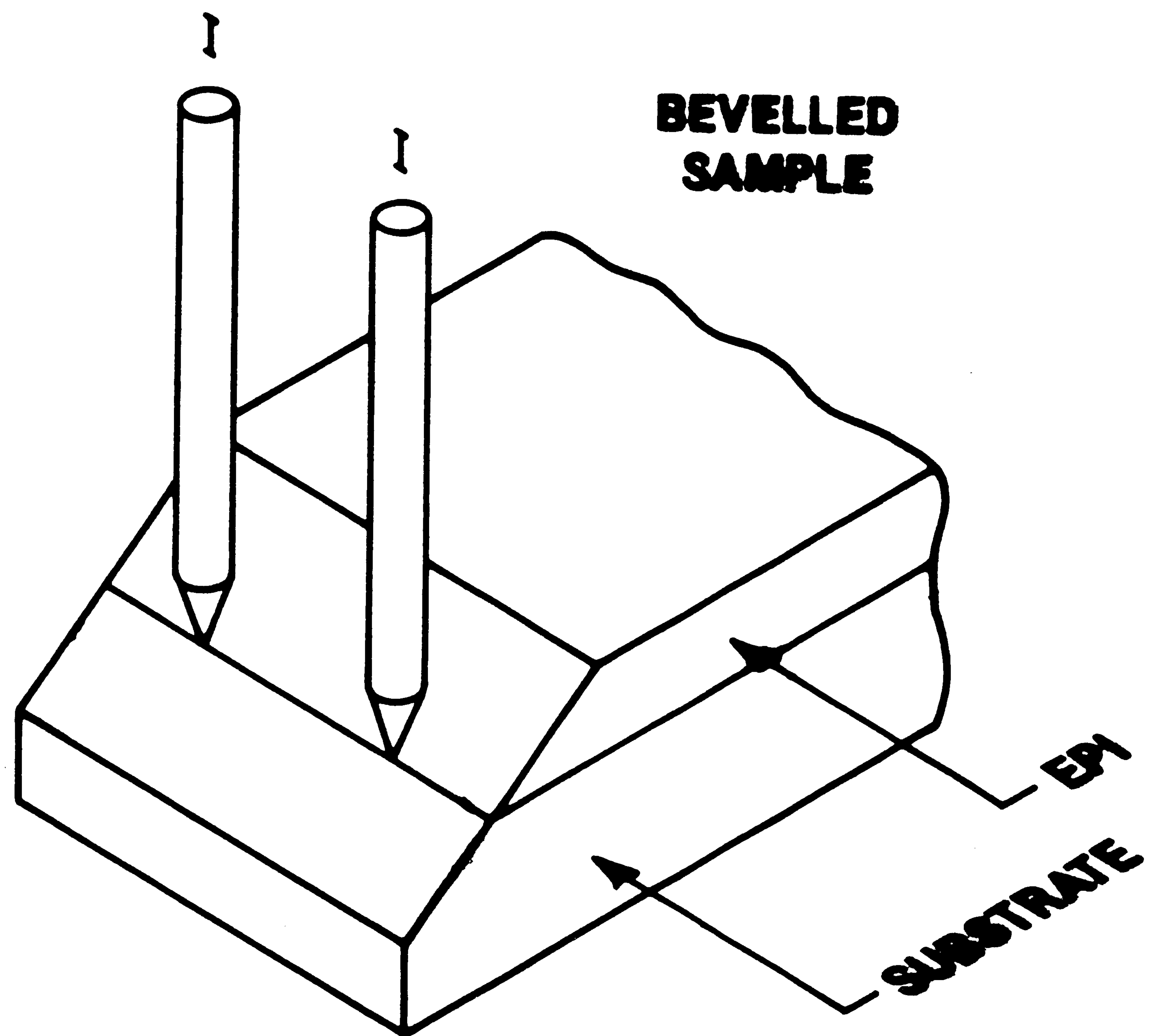

Figure 3. Spreading resistance technique

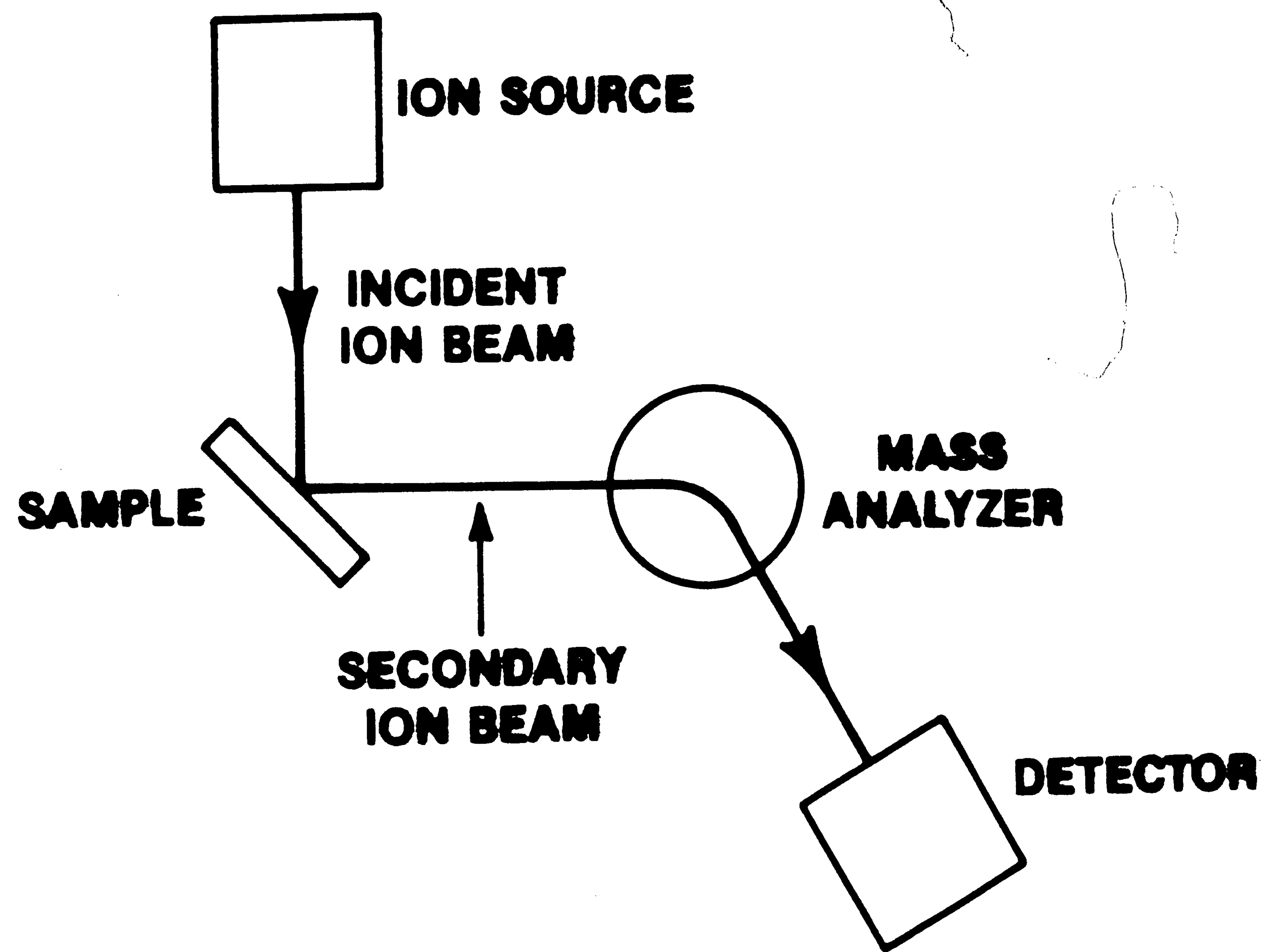

Figure 4. Schematic of SIMS technique

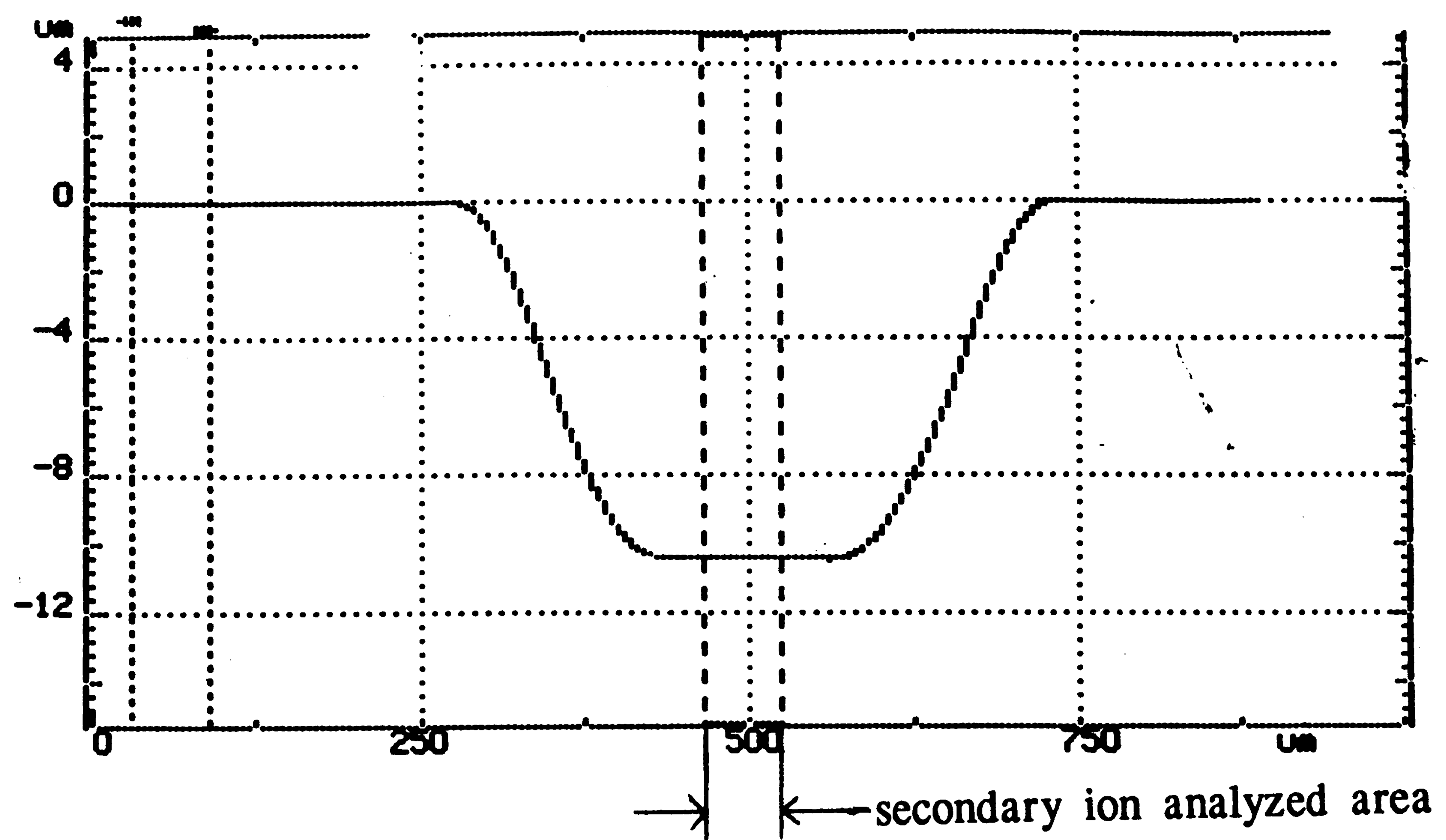

Figure 5. SIMS sample area

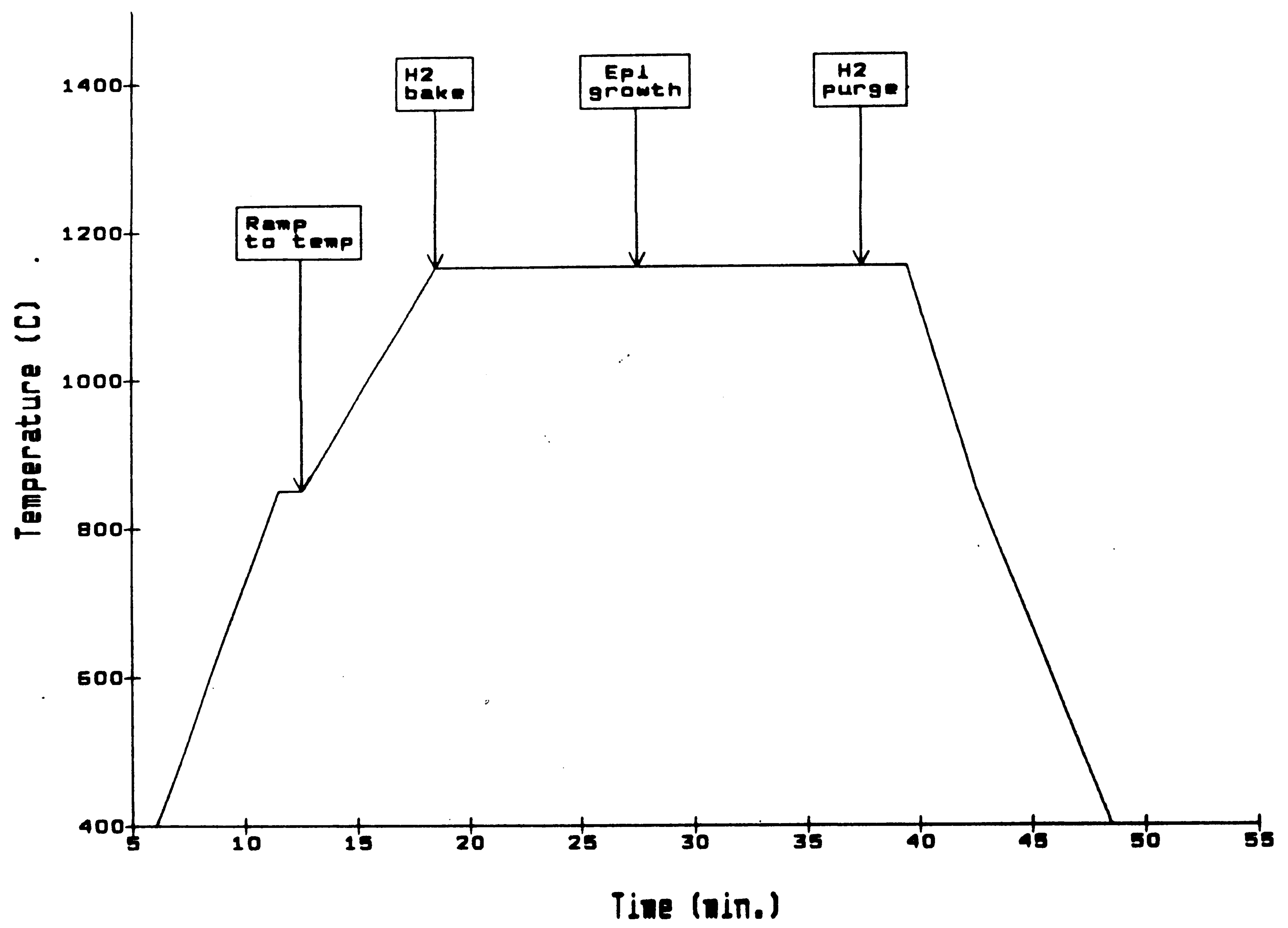

Figure 6. Epi processing sequence

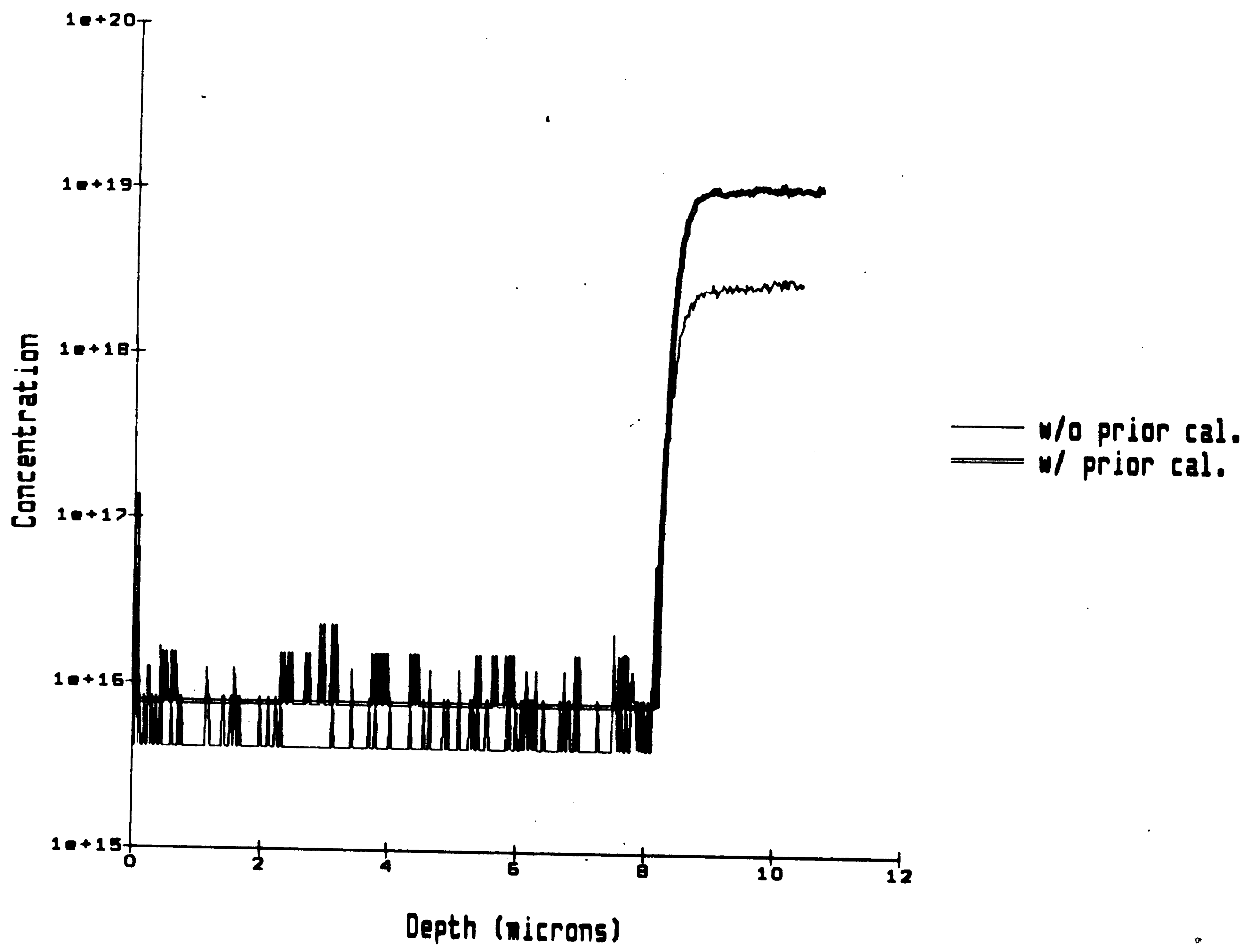

Figure 7. SIMS 1050°C sample analyses with and without prior calibration

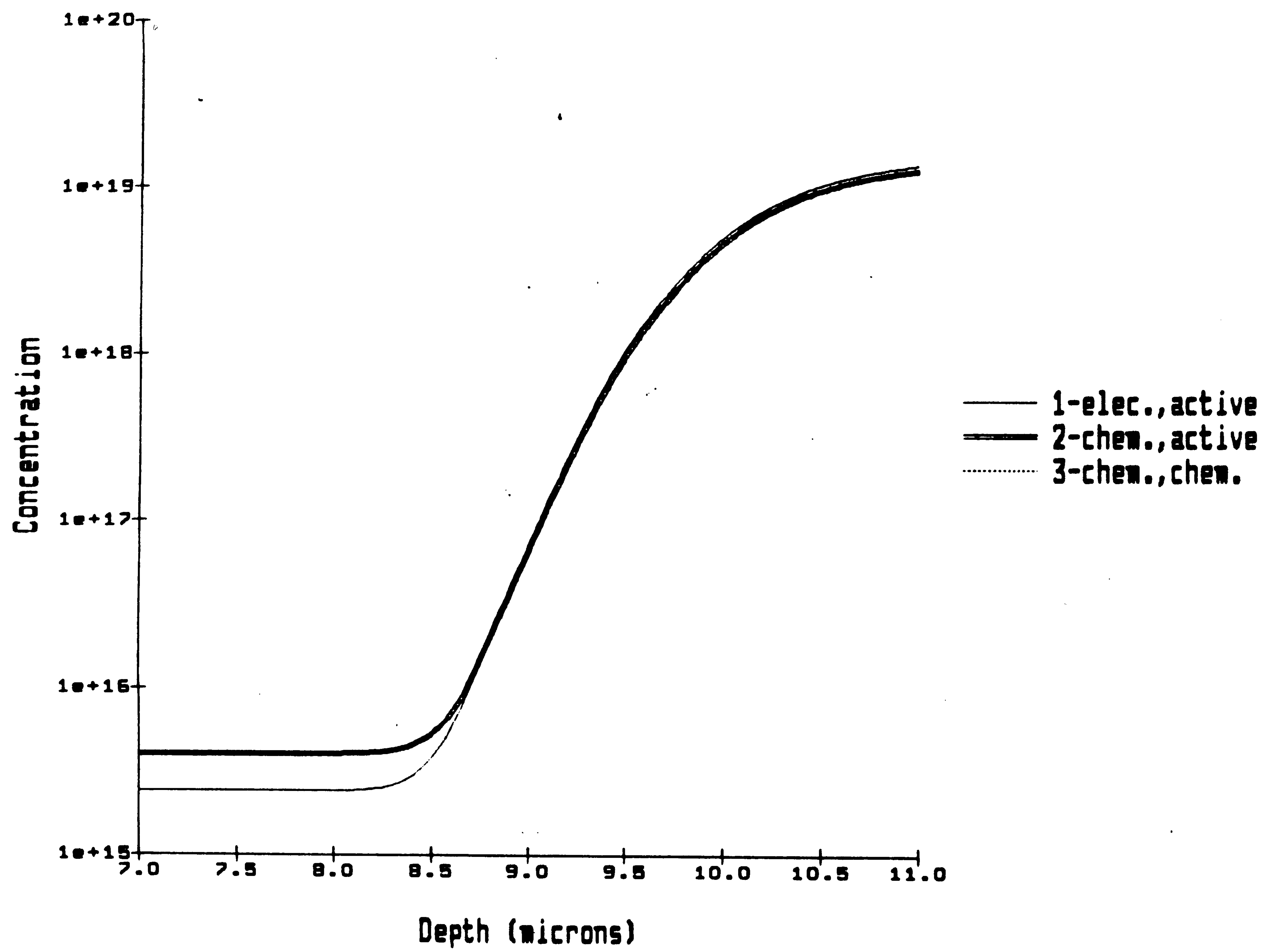

Figure 8. Simulator variation with concentration input and output request

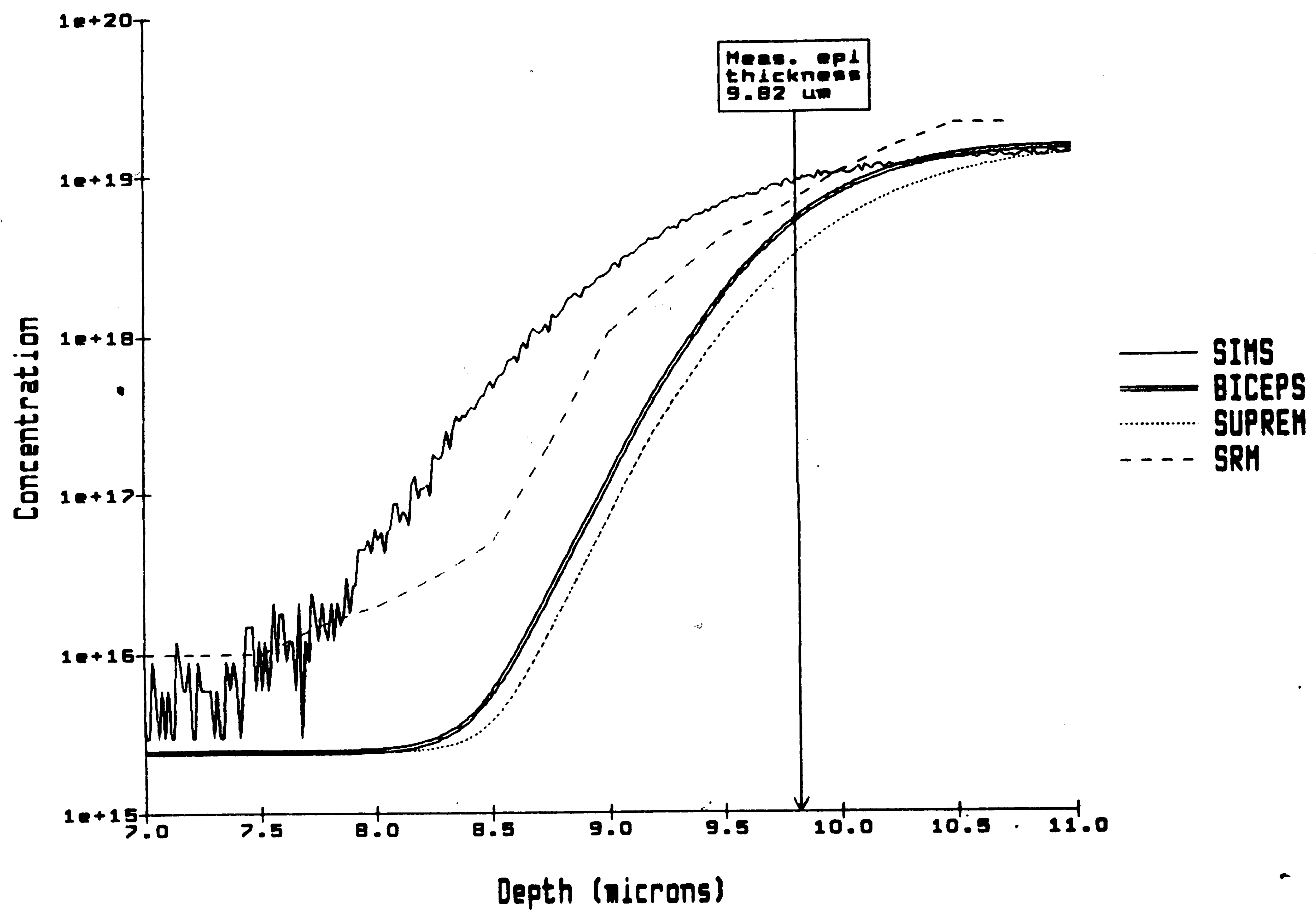

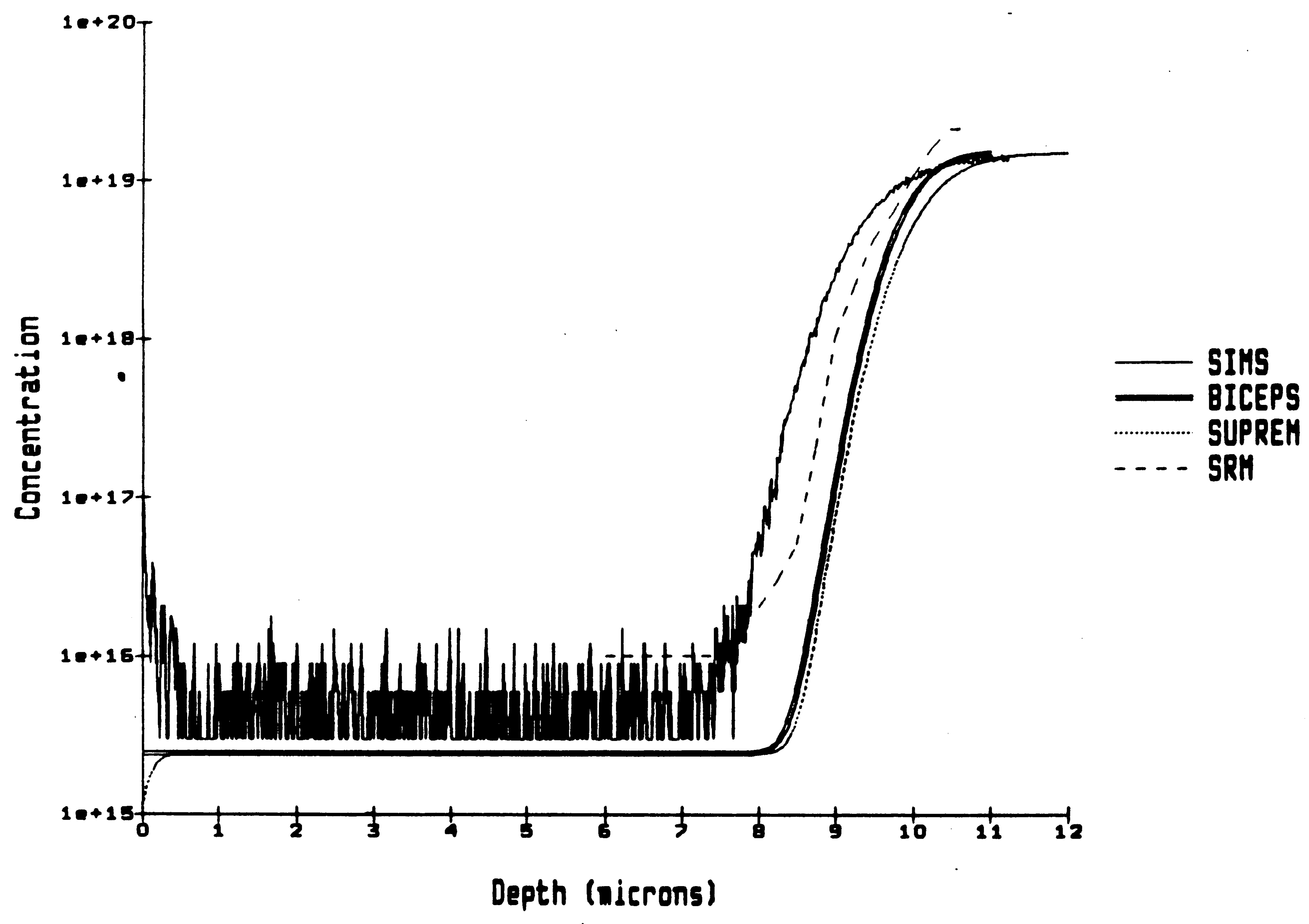

Figure 9. Doping profiles for 1200° C epi

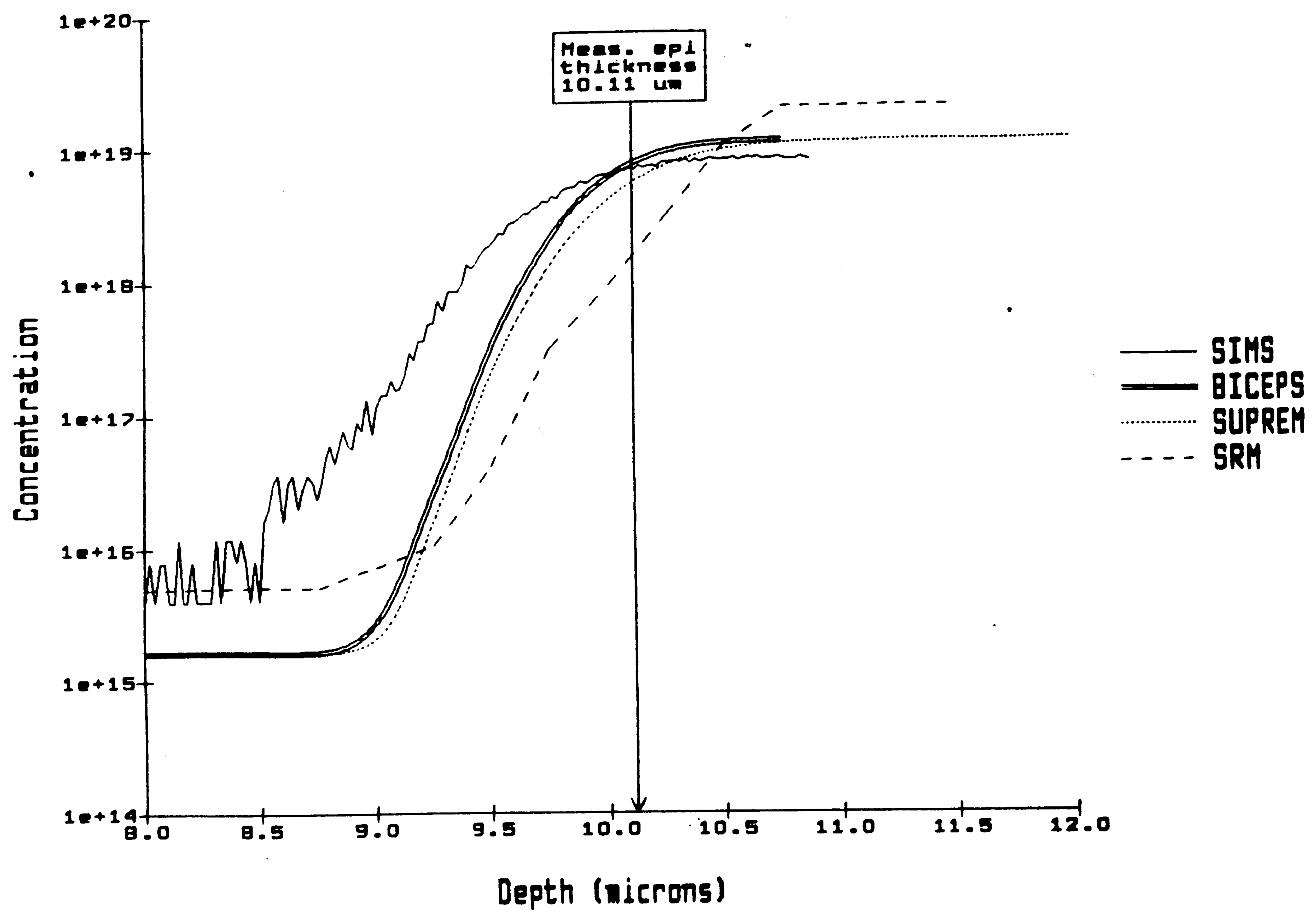

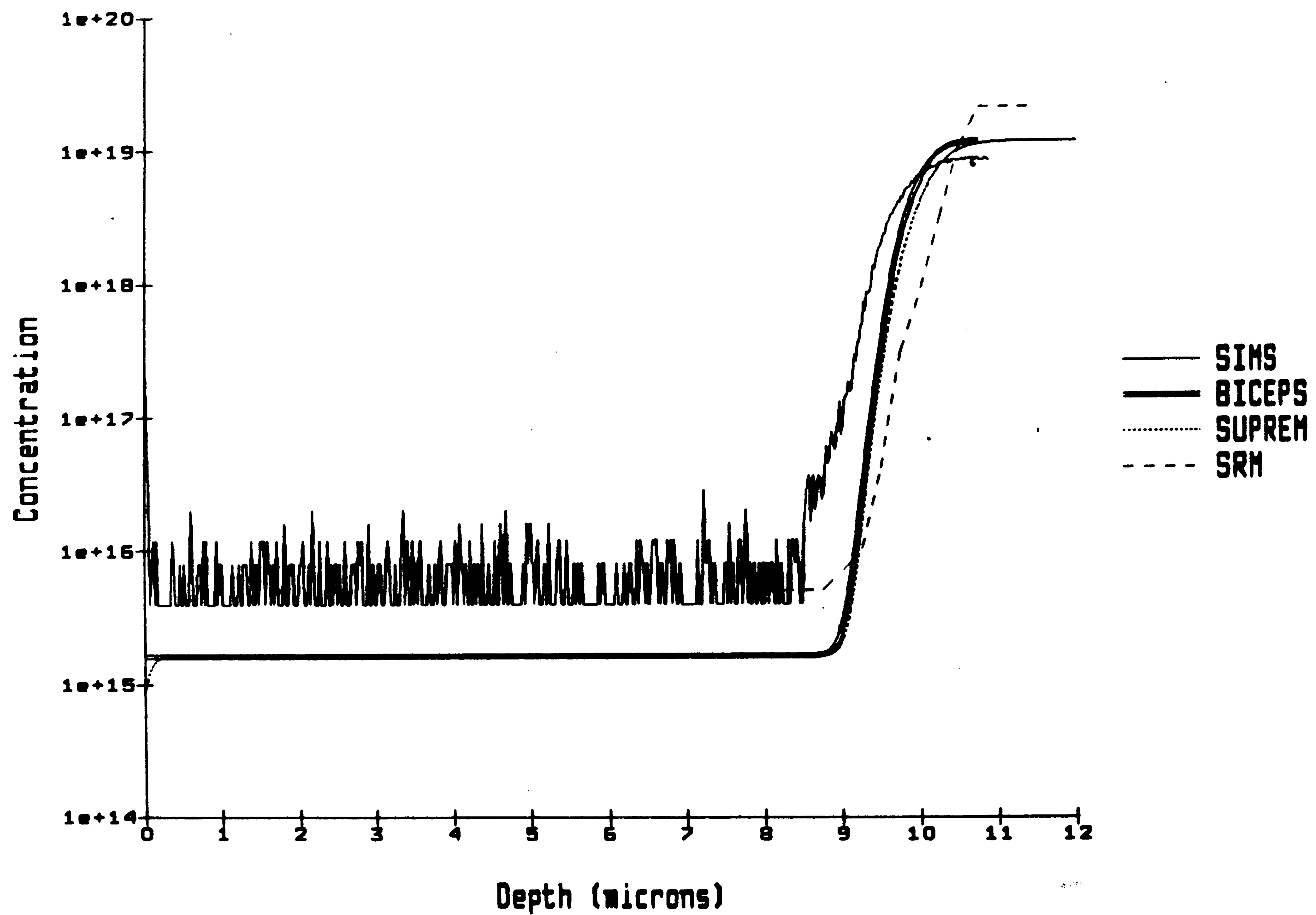

Figure 10. Doping profiles for 1150° C epi

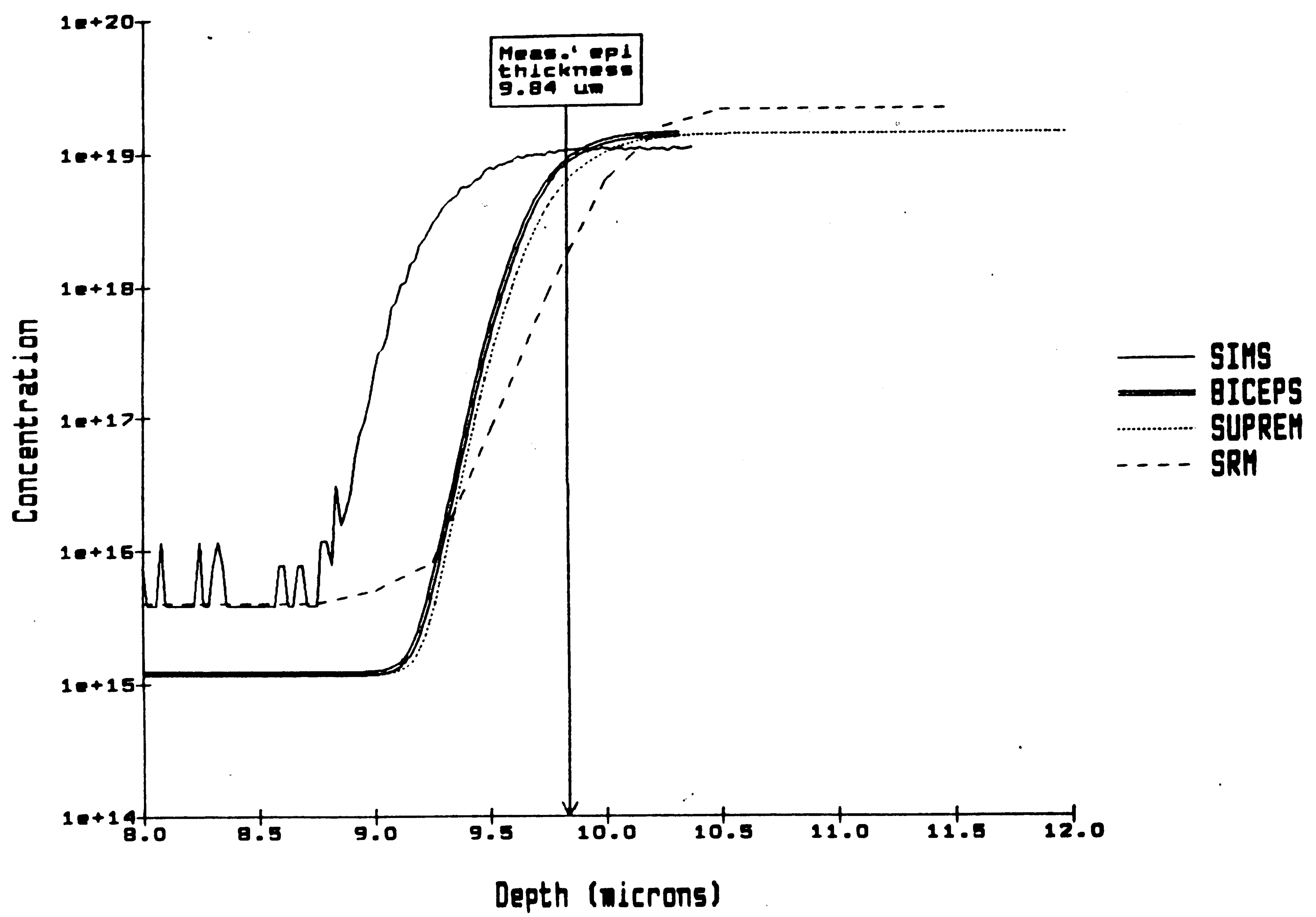

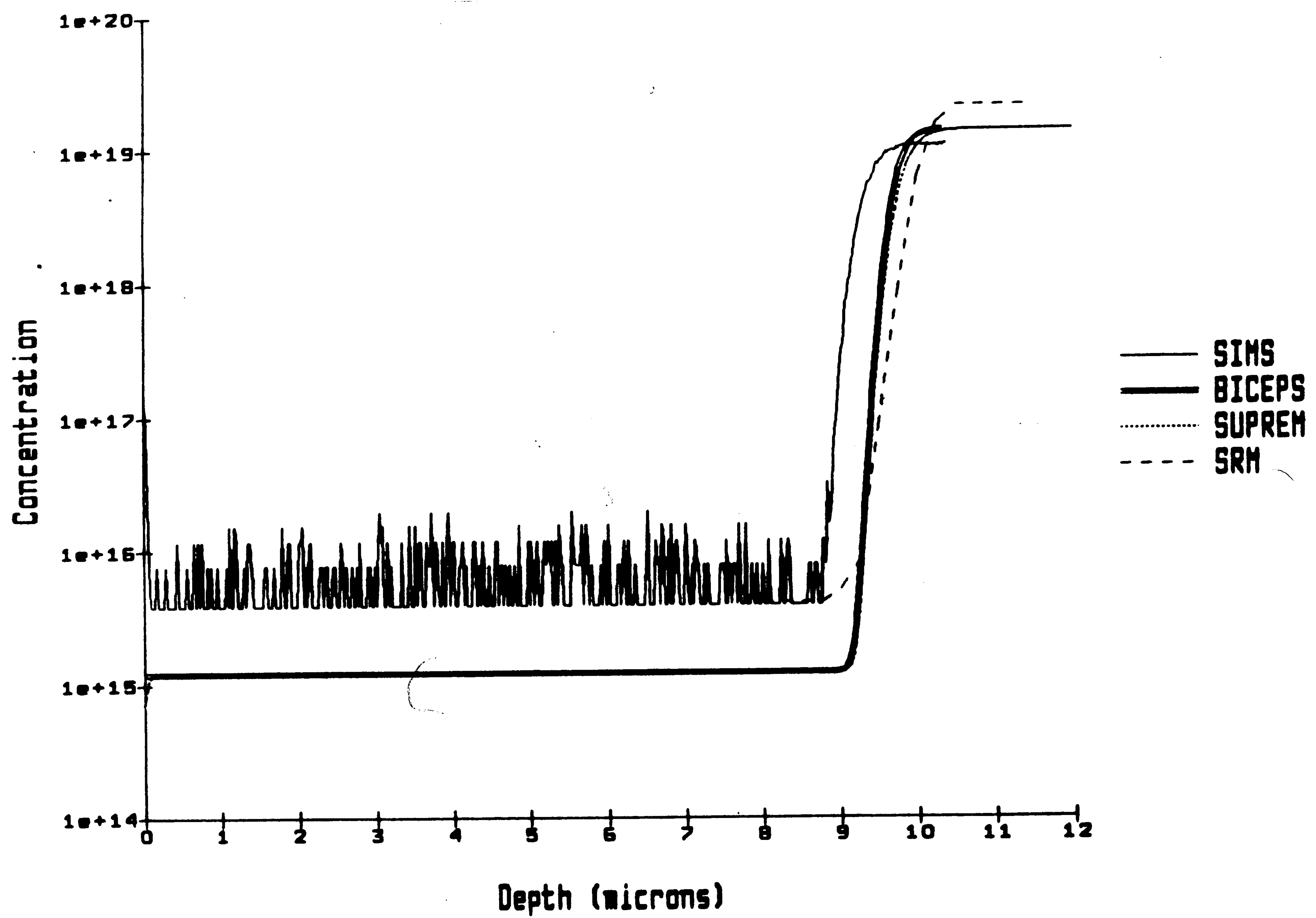

Figure 11. Doping profiles for 1100° C epi

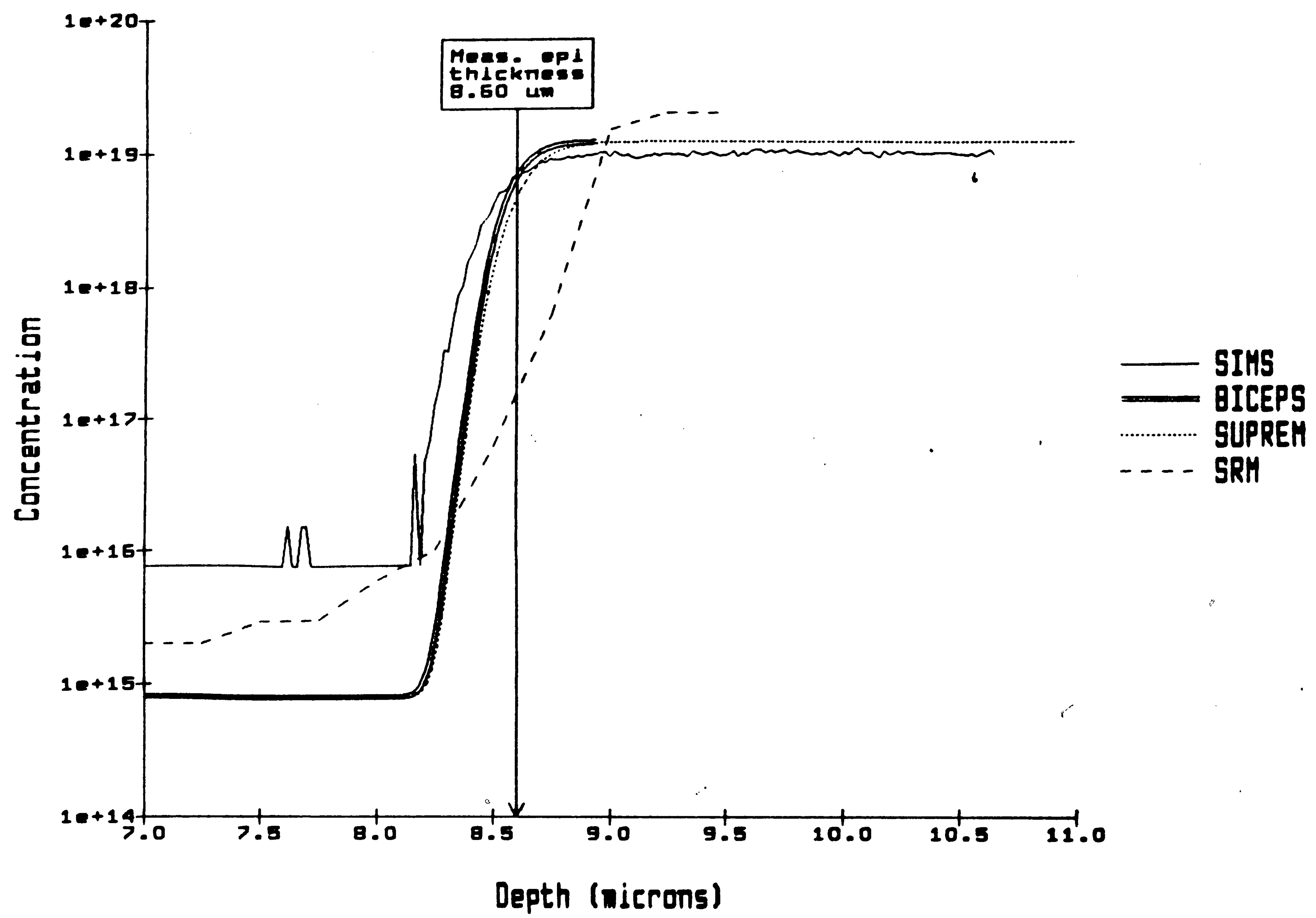

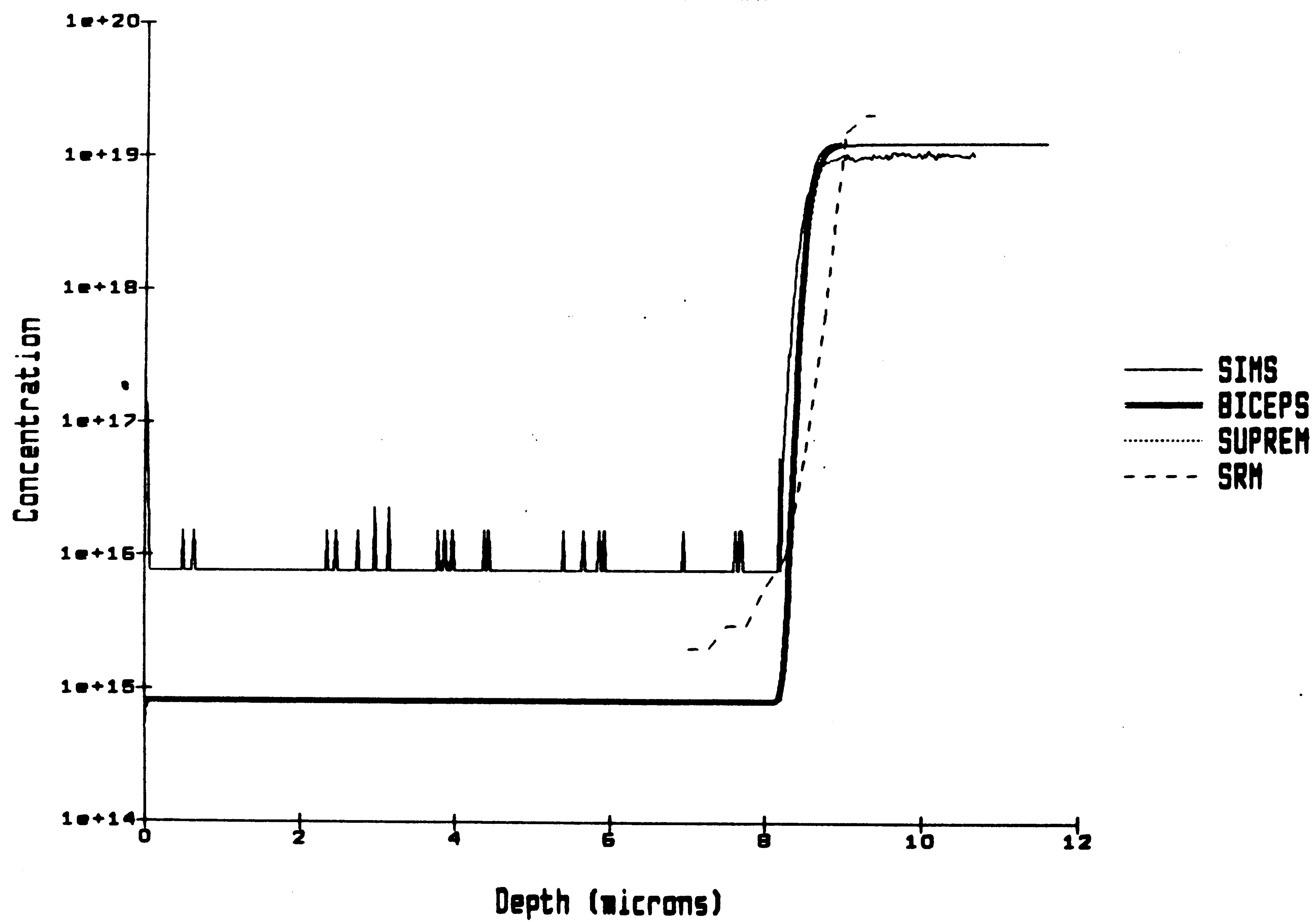

Figure 12. Doping profiles for 1050° C epi

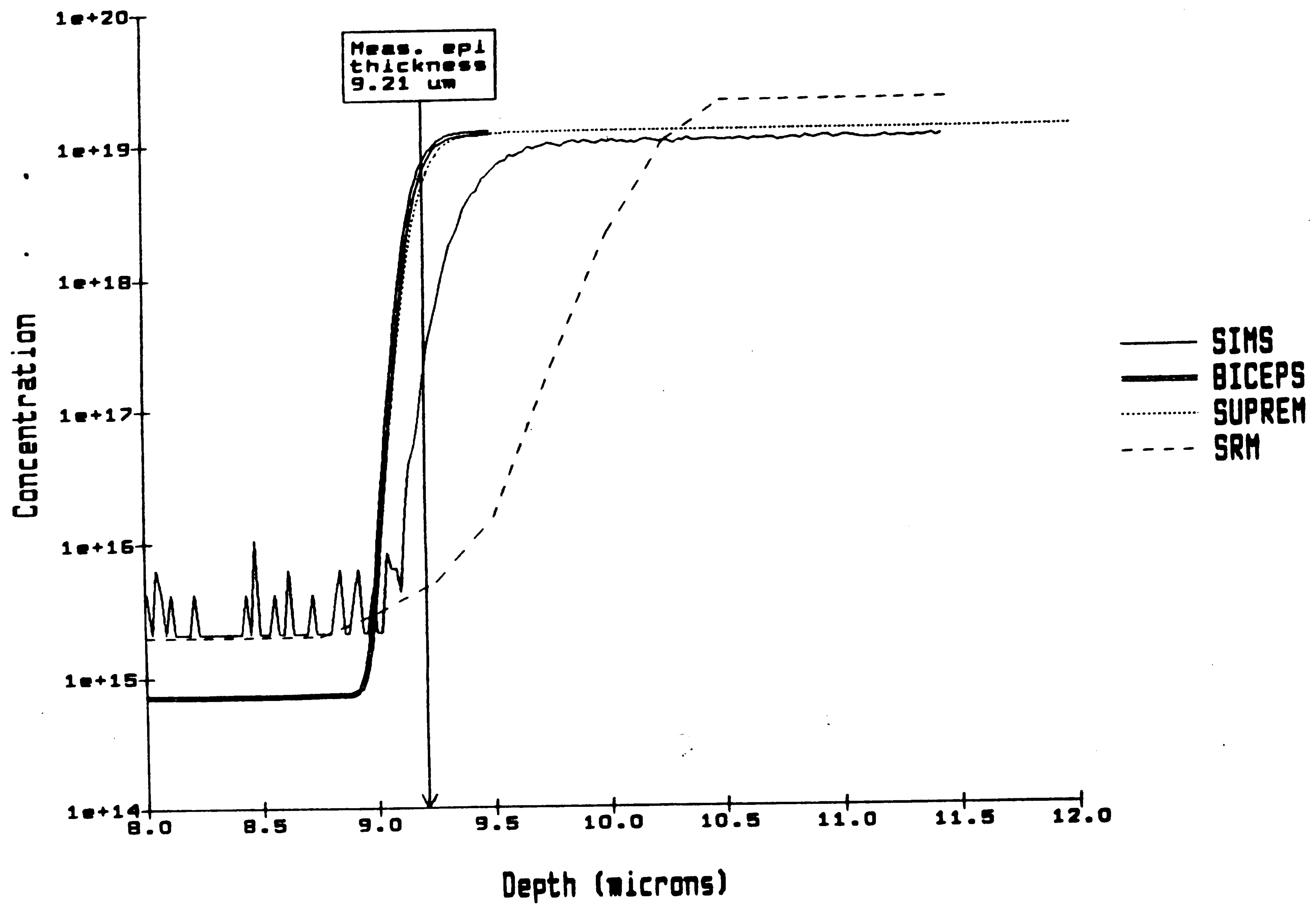

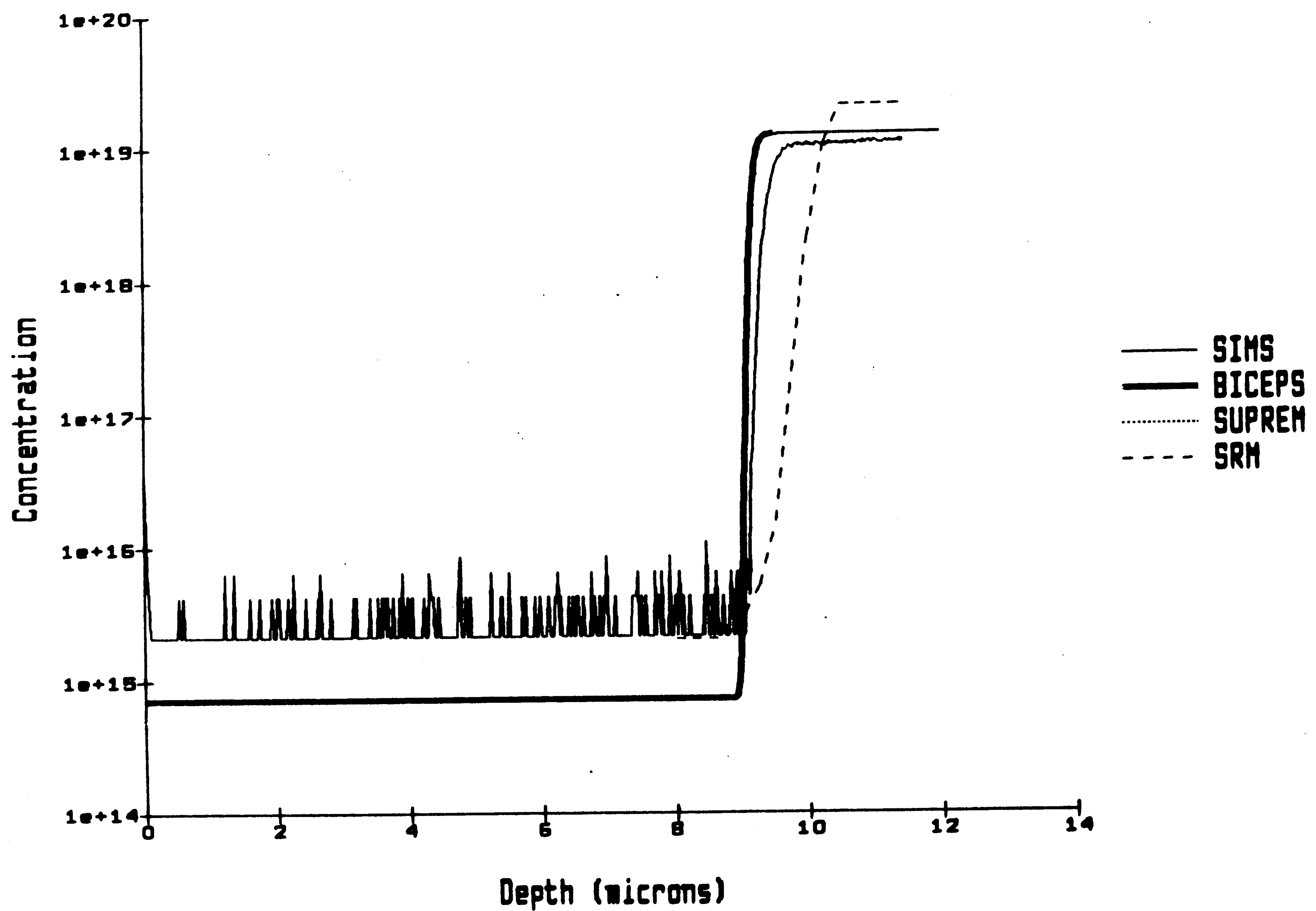

Figure 13. Doping profiles for 1000° C epi

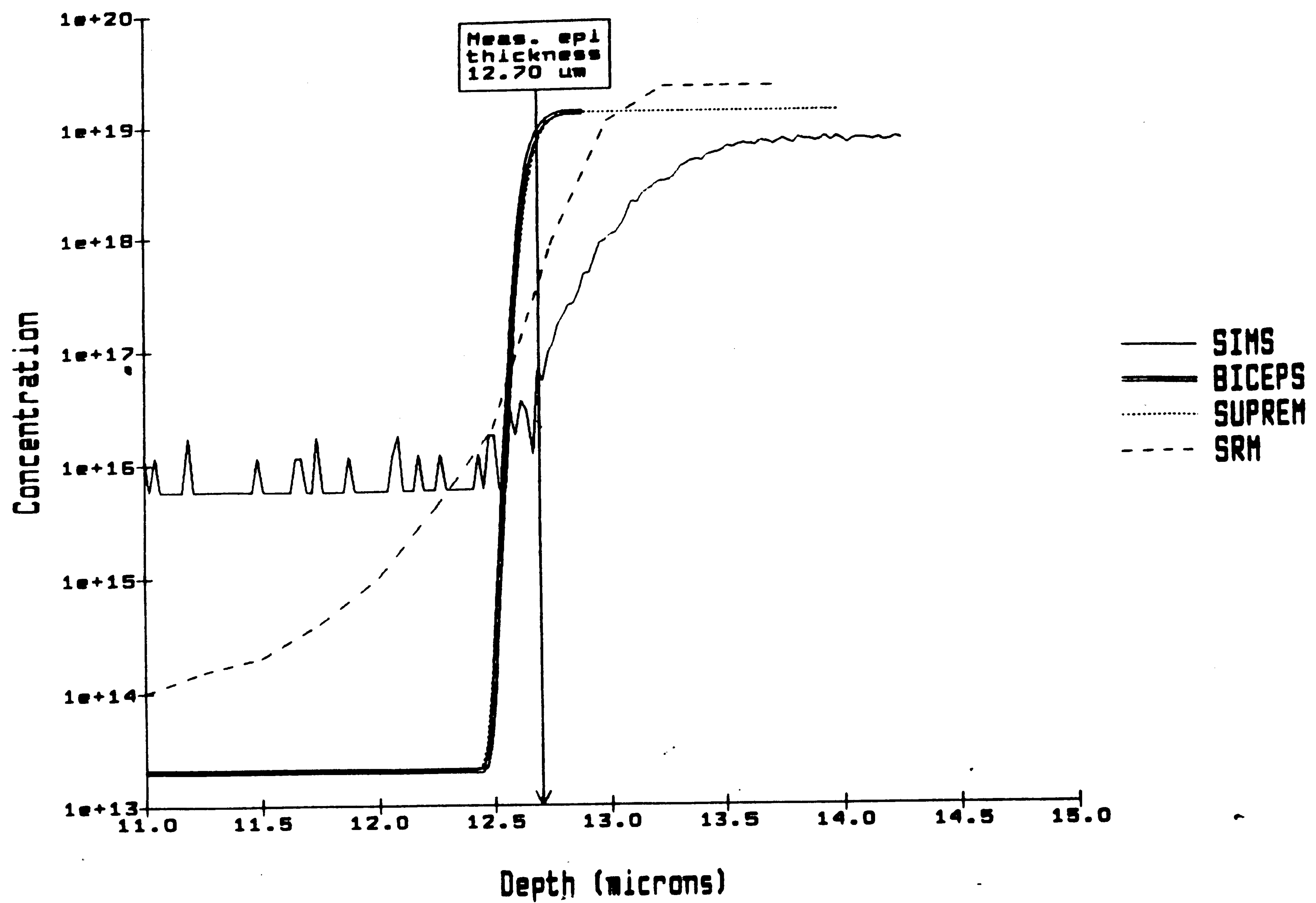

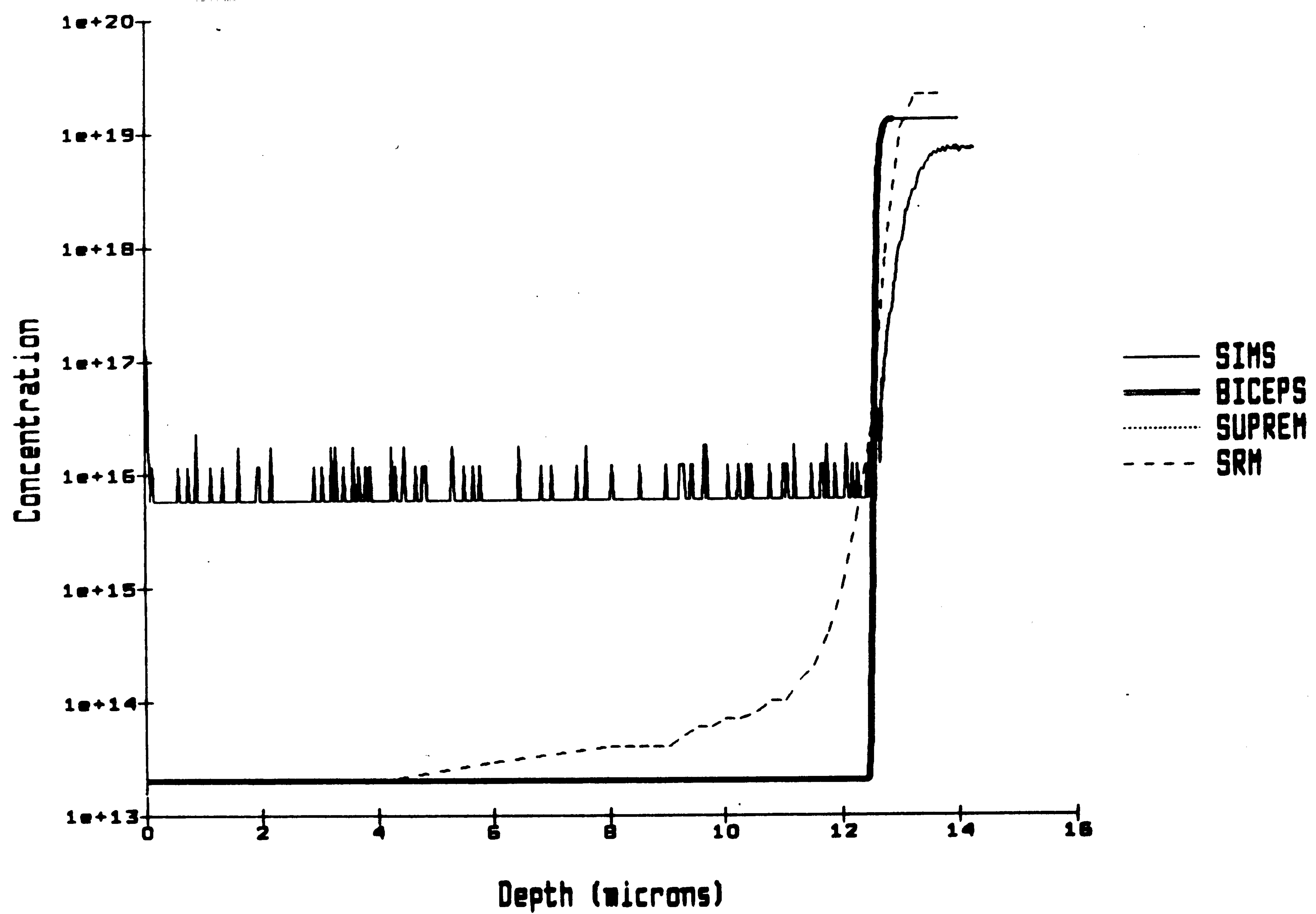

Figure 14. Doping profiles for 950° C epi

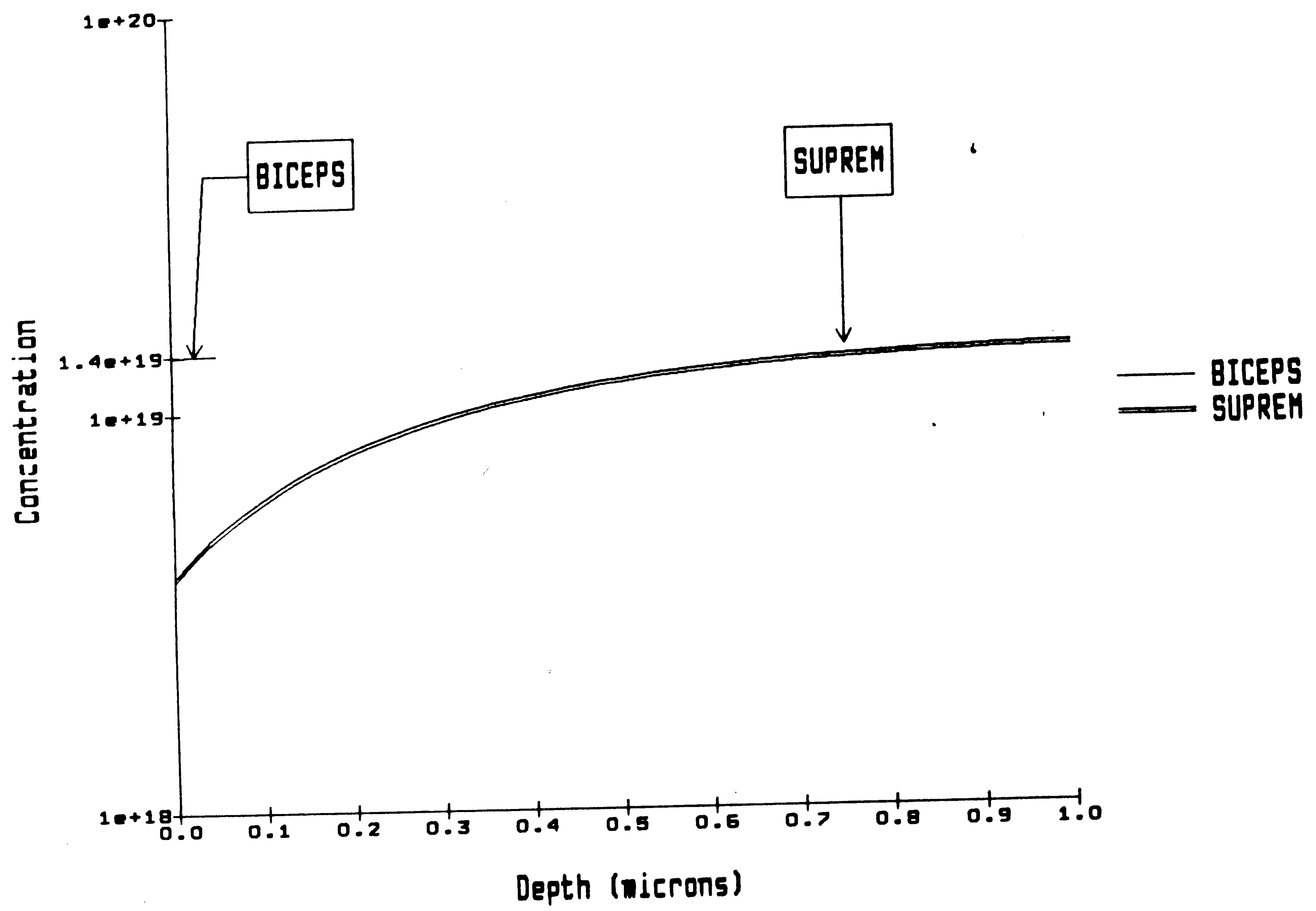

Figure 15. Simulator out-diffusion comparison

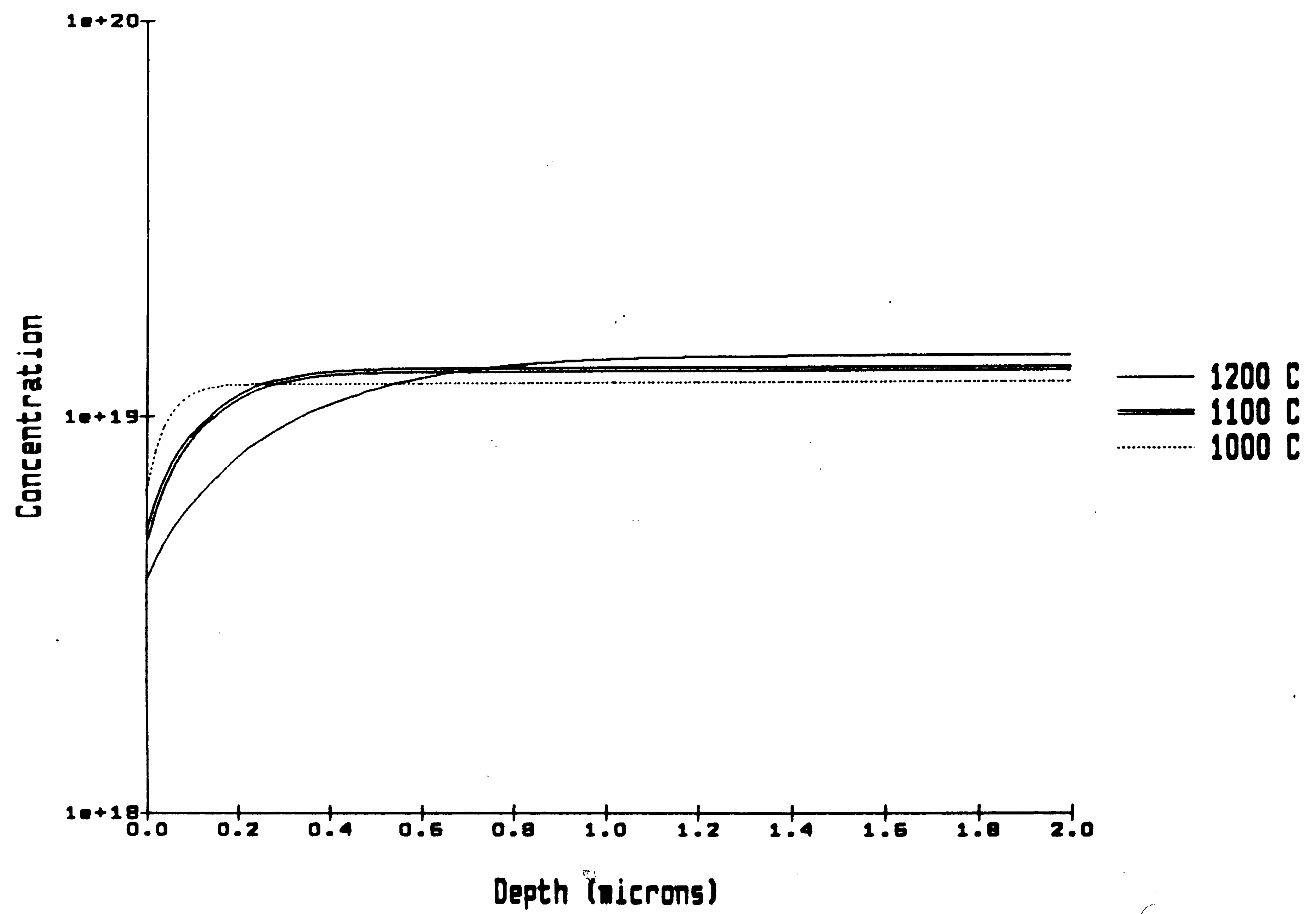

Figure 16. SUPREM out-diffusion effect as a function of temperature

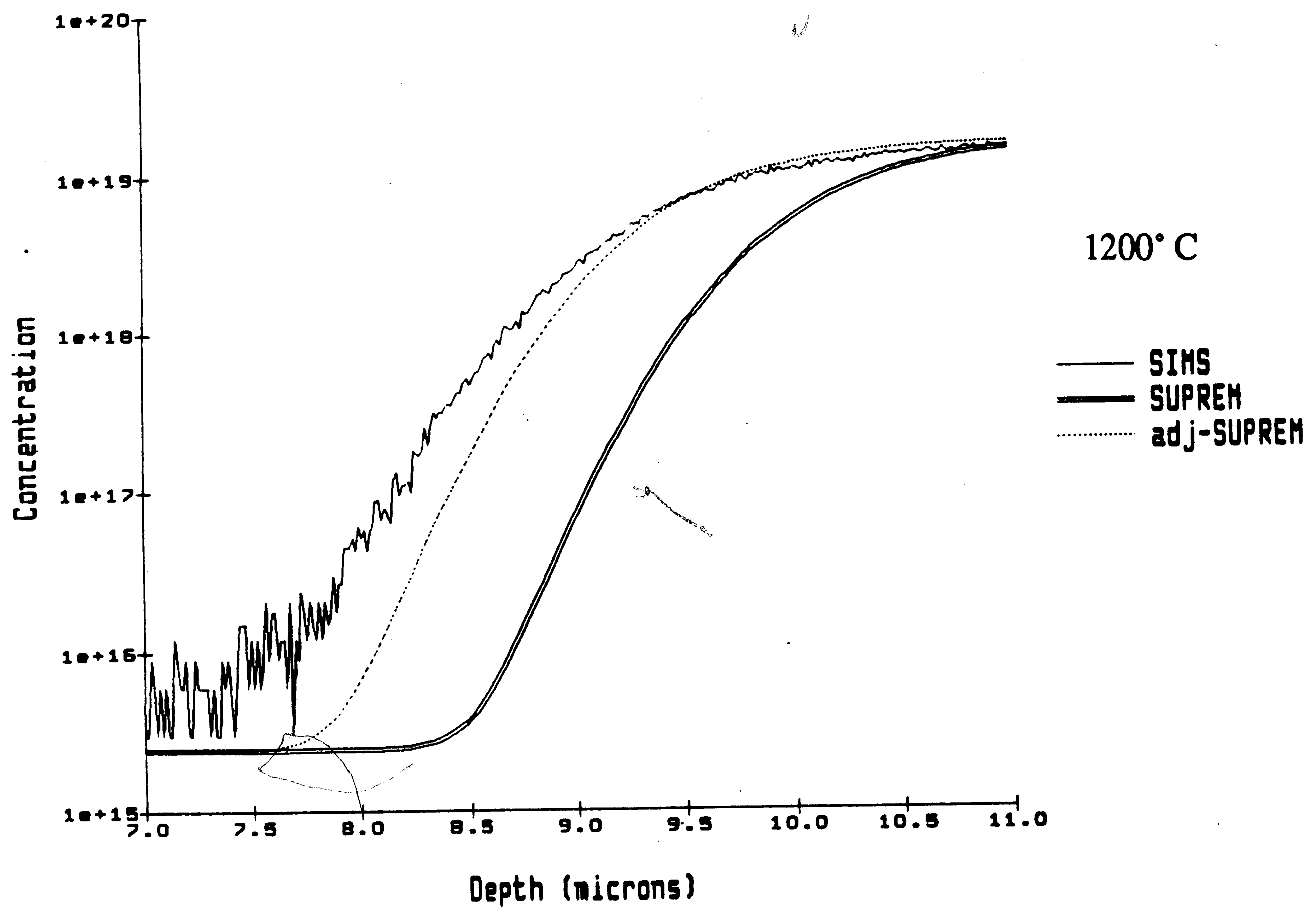

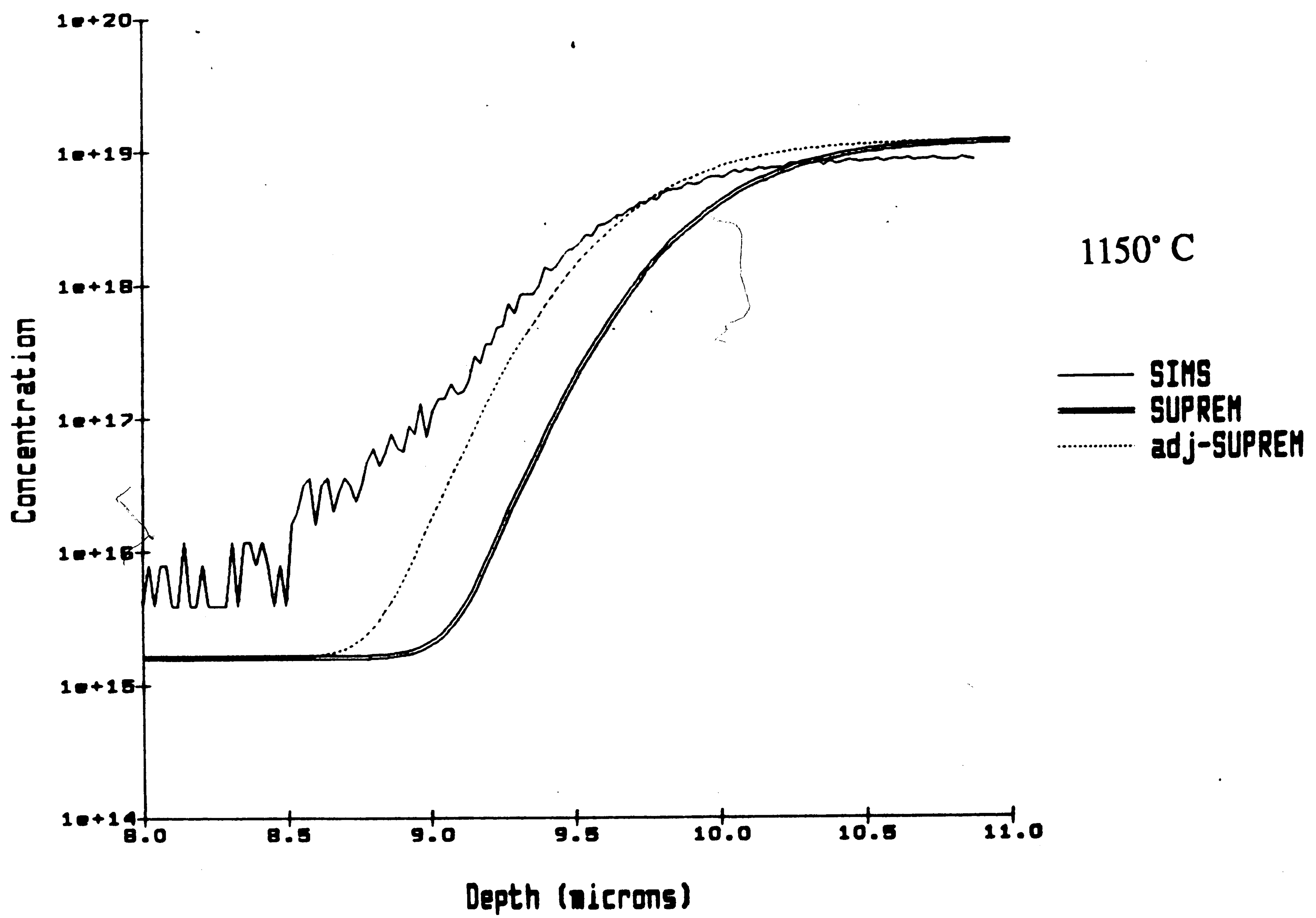

Figure 17. Simulator profile shift at defined 50% interface for 1200 and 1150° C

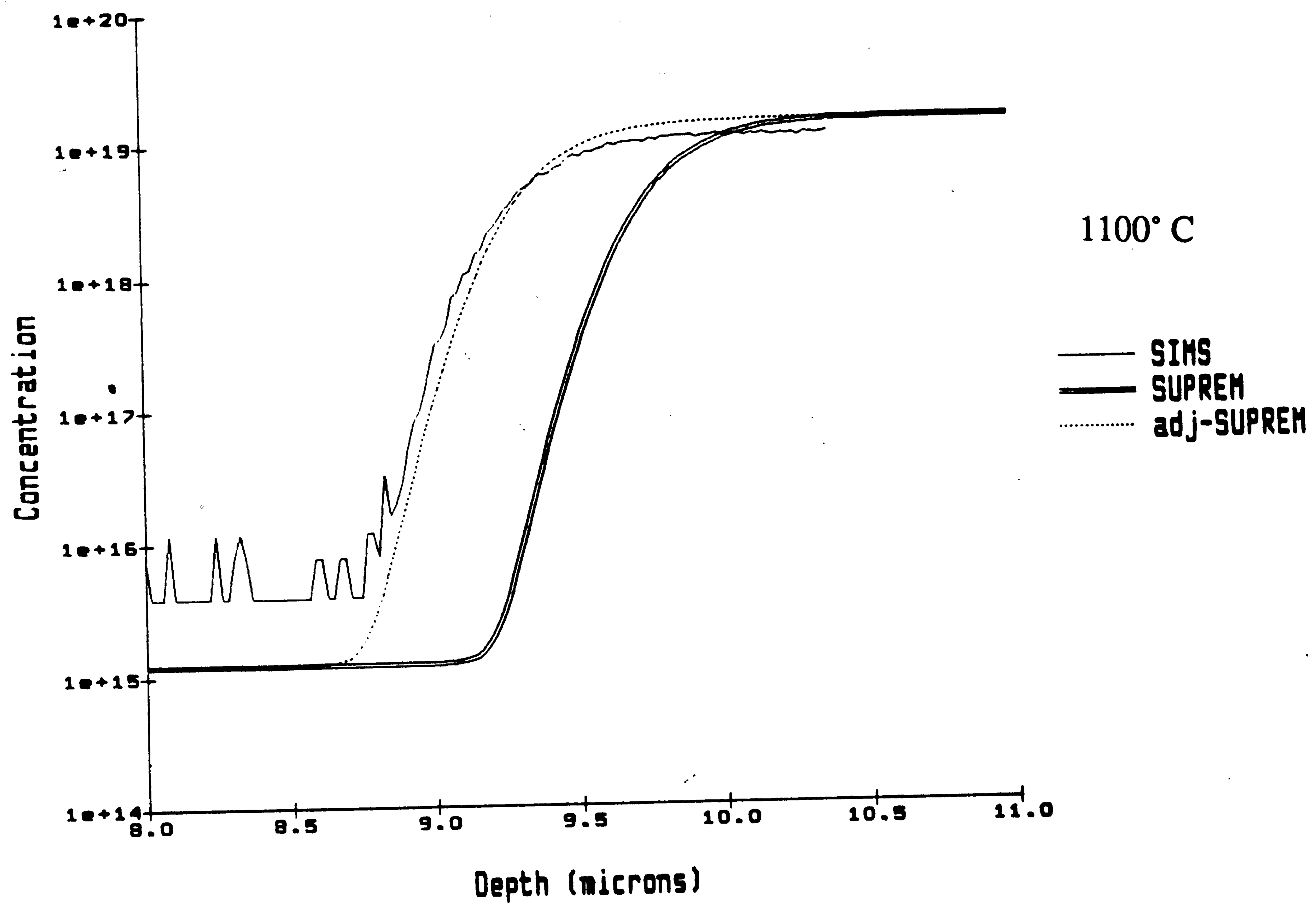

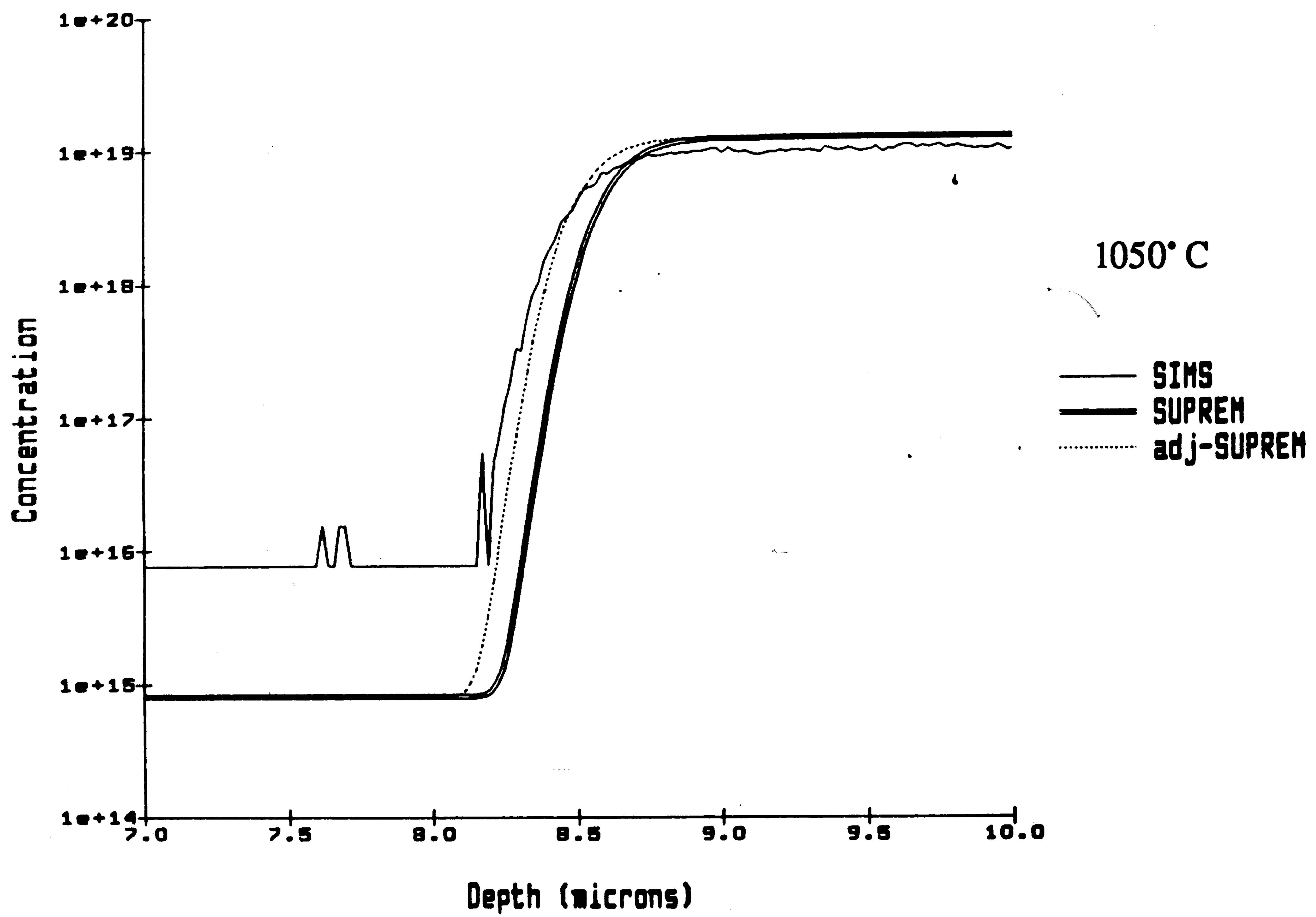

Figure 18. Simulator profile shift at defined 50% interface for 1100 and 1050° C

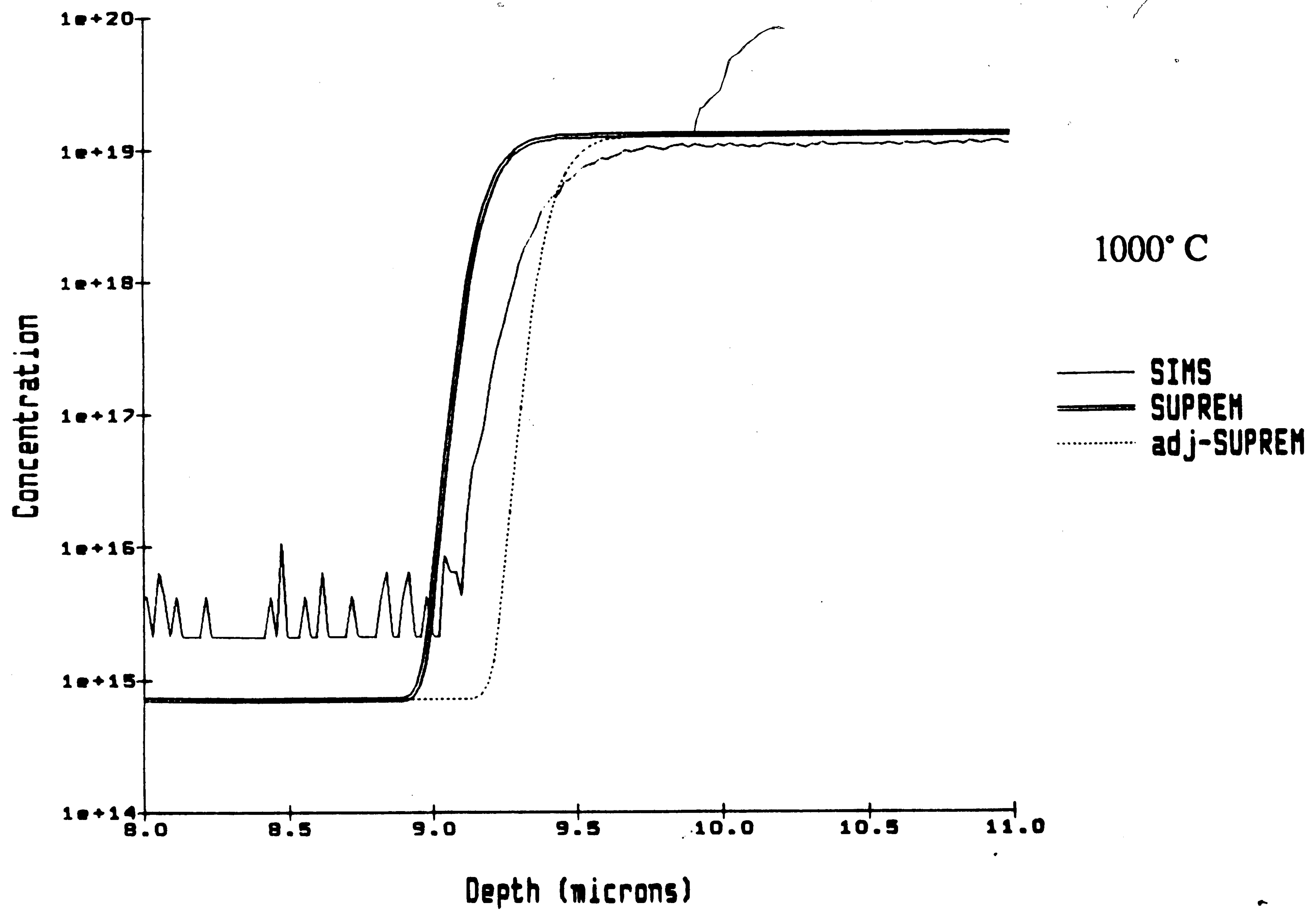

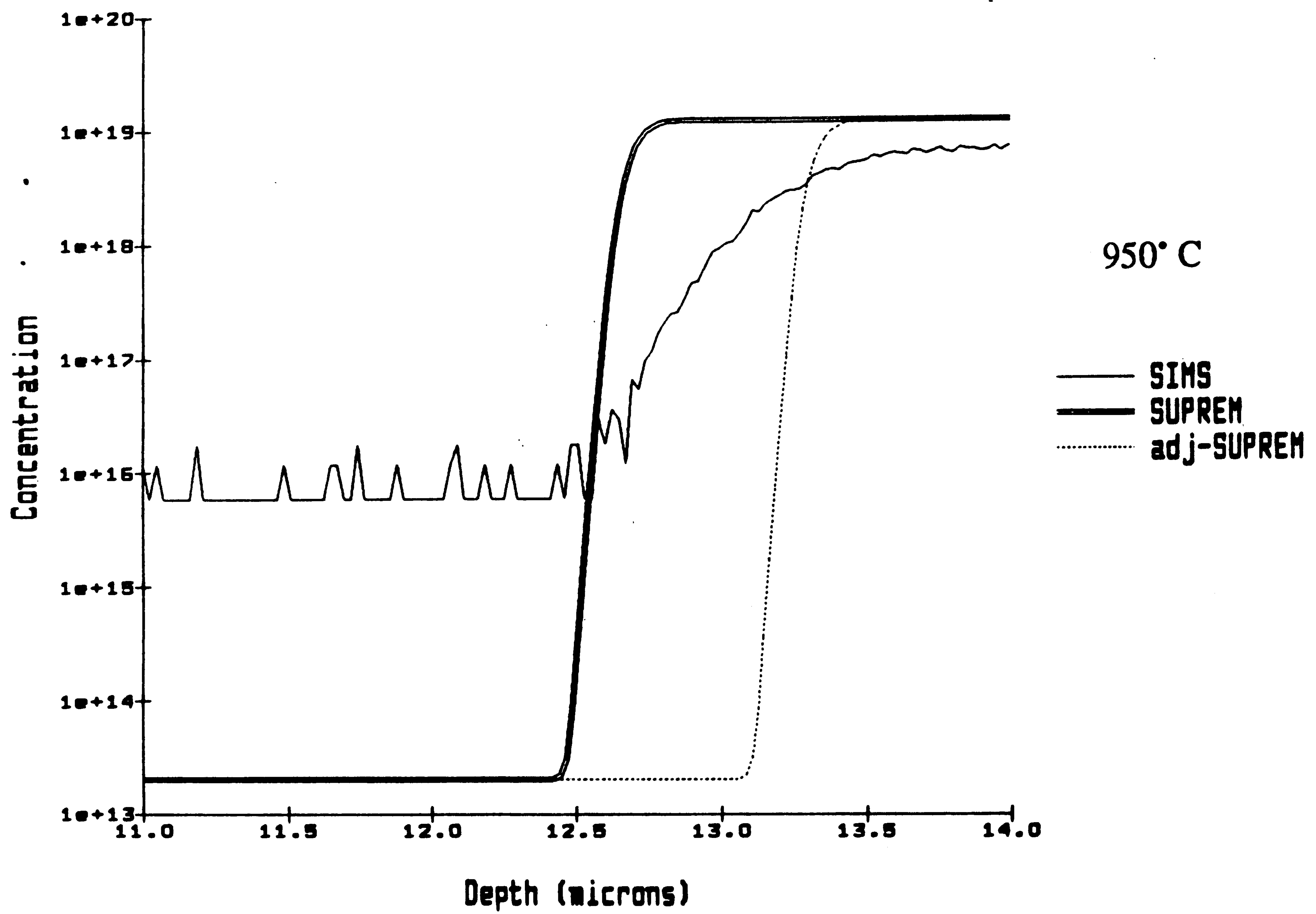

Figure 19. Simulator profile shift at defined 50% interface for 1000 and 950° C

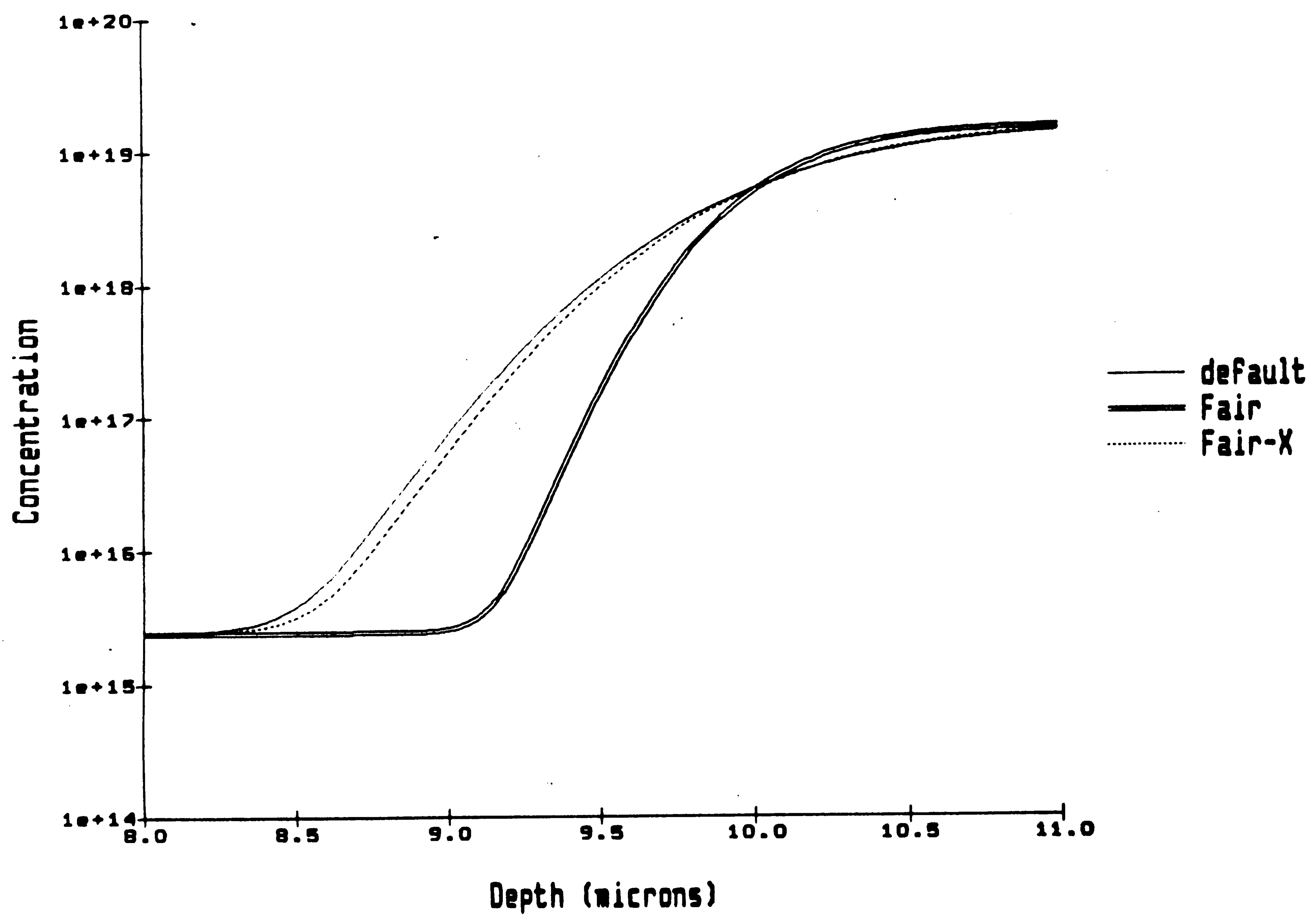

Figure 20. 1200 °C SUPREM simulation using Fair model parameters, effective diffusivity with Fair parameters (Fair-X), and default SUPREM parameters

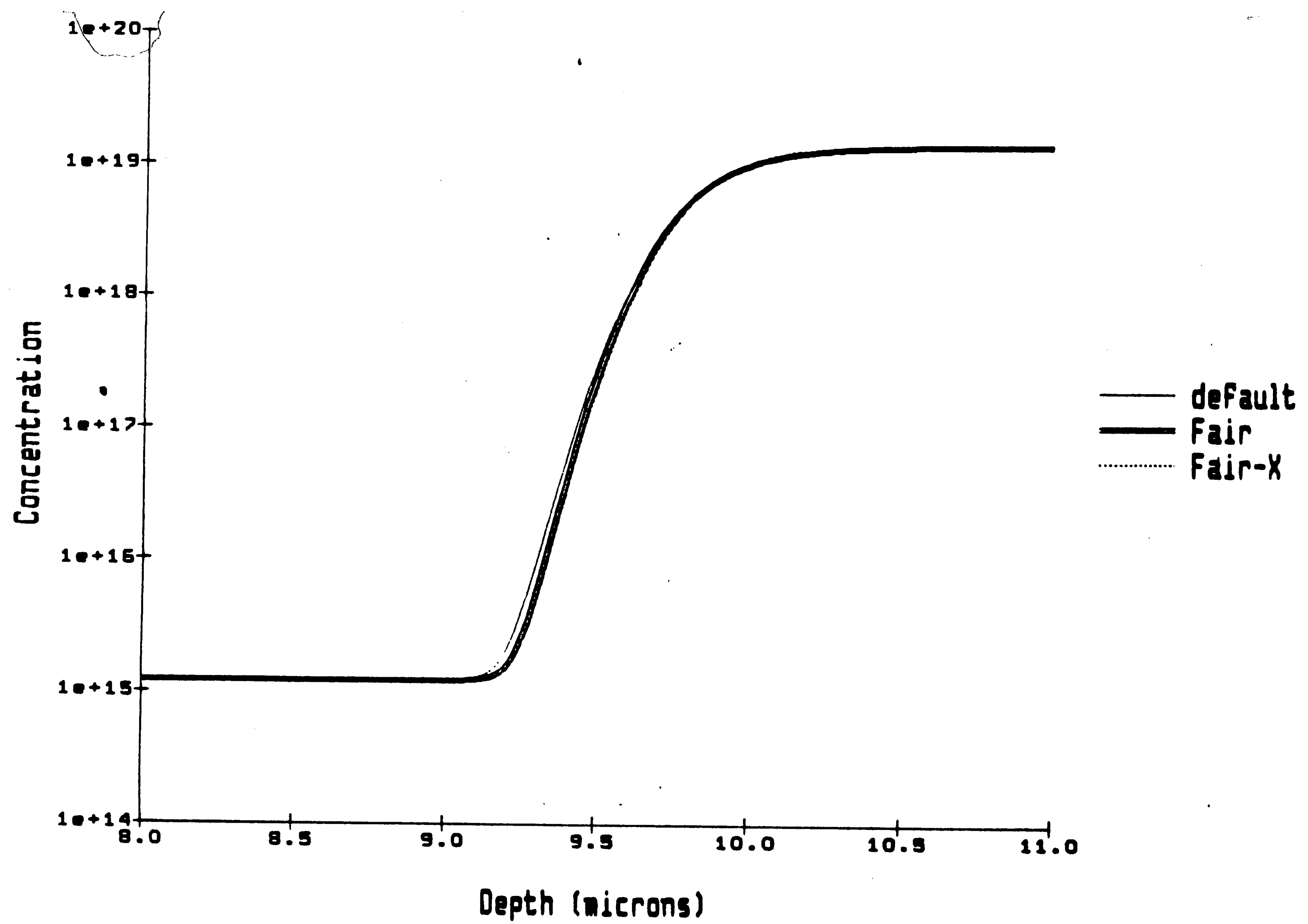

Figure 21. 1100 °C SUPREM simulation using Fair model parameters, effective diffusivity with Fair parameters (Fair-X), and default SUPREM parameters

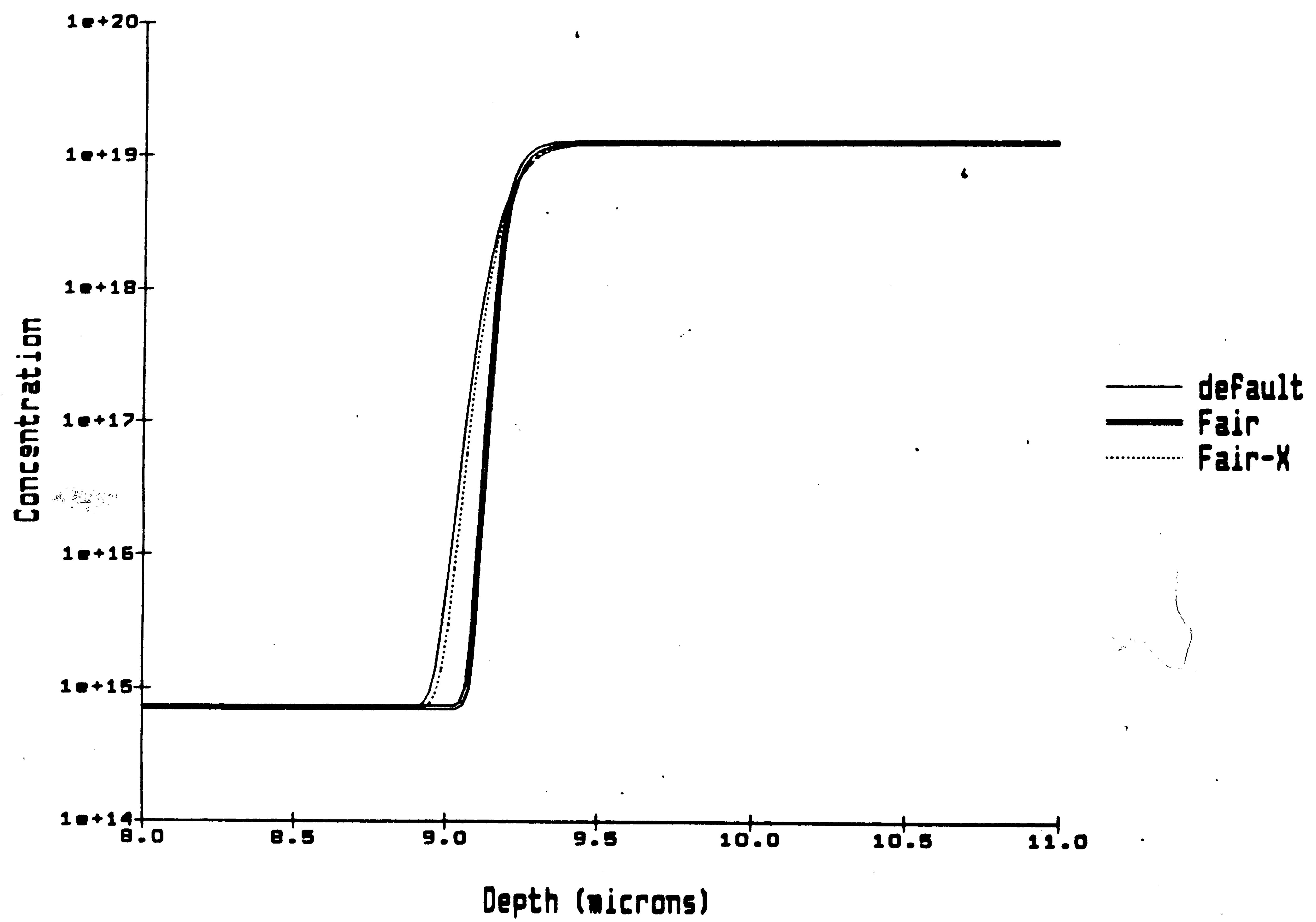

Figure 22. 1000 °C SUPREM simulation using Fair model parameters, effective diffusivity with Fair parameters (Fair-X), and default SUPREM parameters

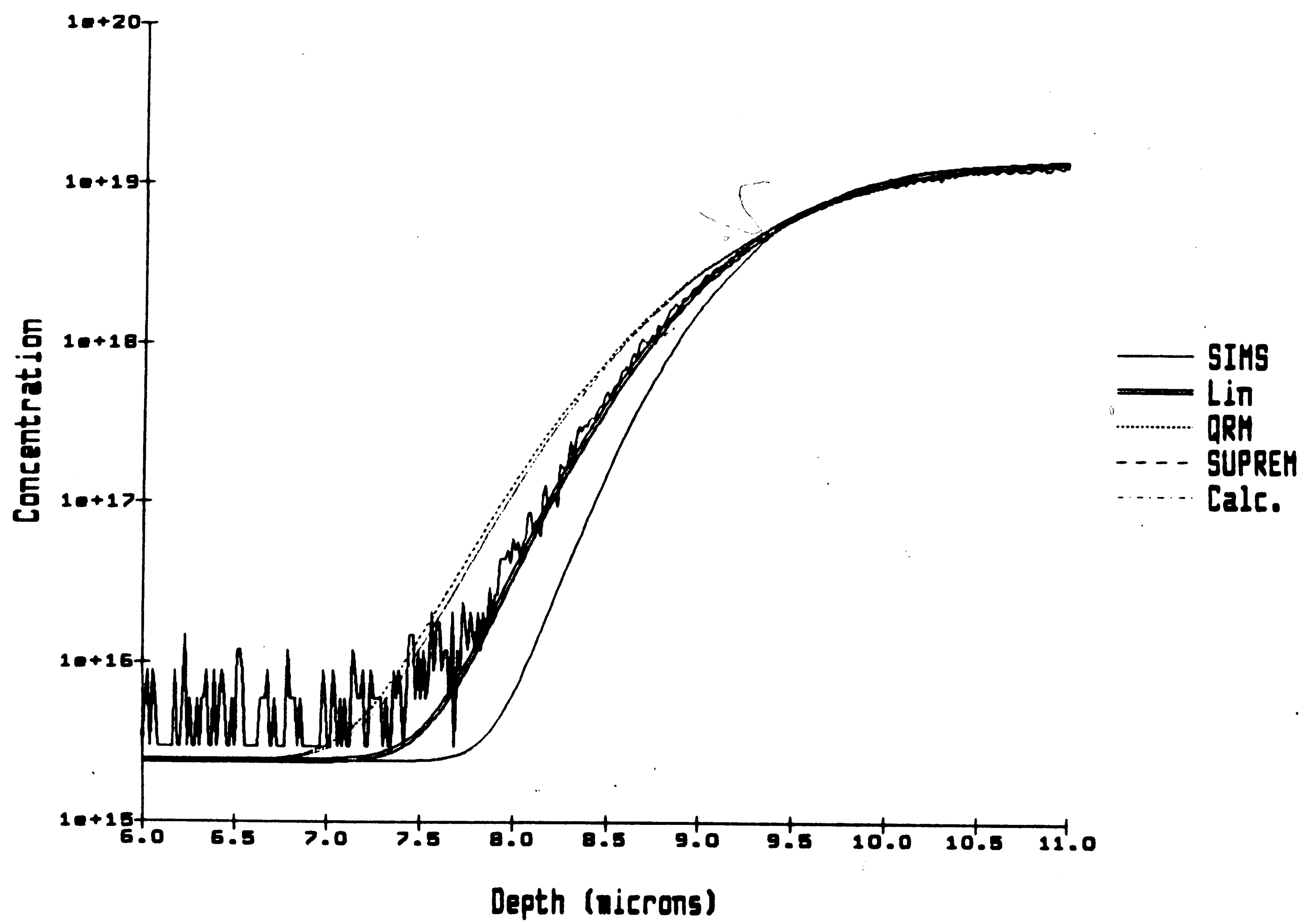

Figure 23. Empirical profiles for 1200° C epi run

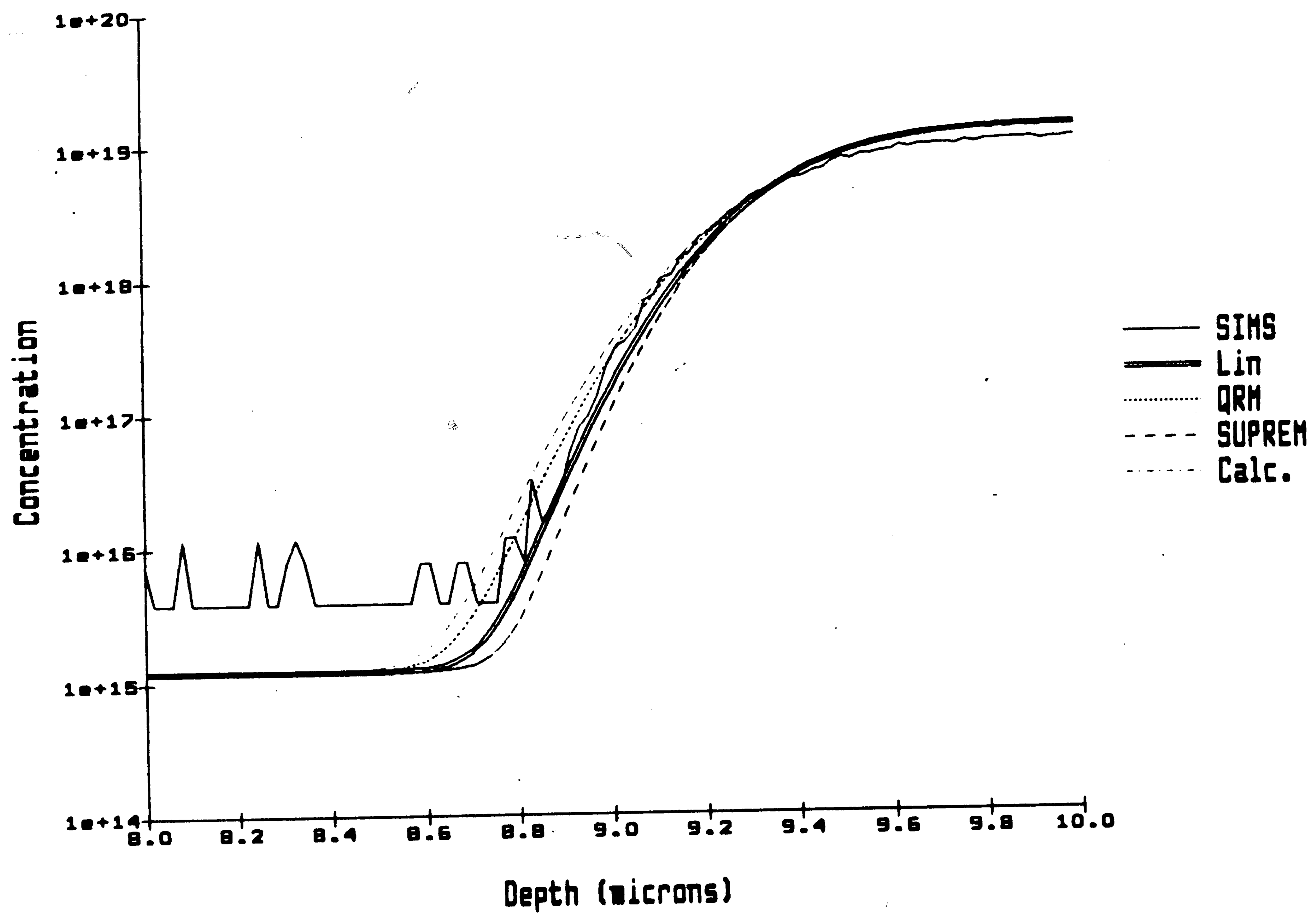

Figure 24. Empirical profiles for 1100° C epi run

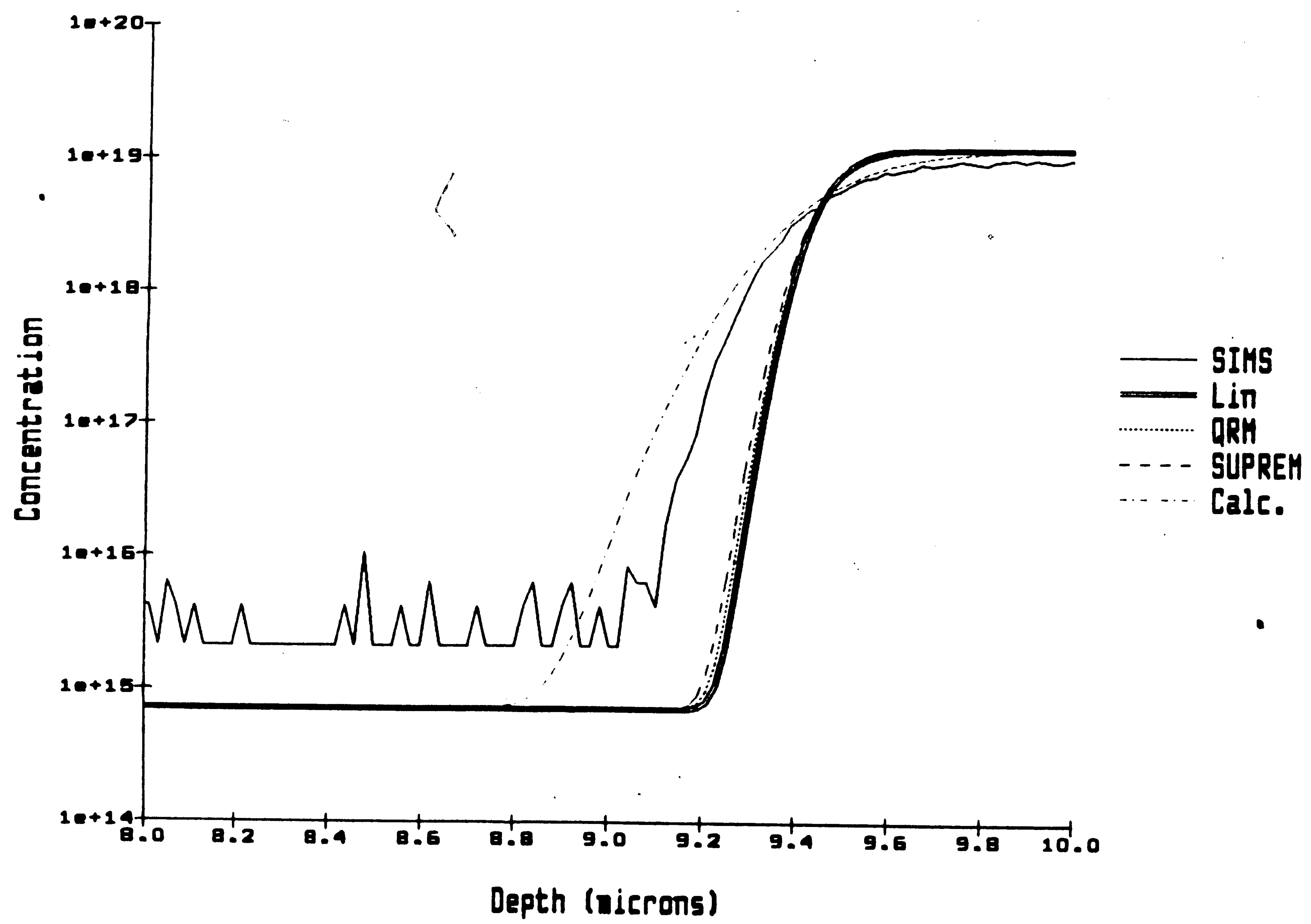

Figure 25. Empirical profiles for 1000° C epi run

REFERENCES

1. Masaahiko Ogirima and Ryokichi Takahashi, "Some Problems and Future Trends in Silicon Epitaxial Technology," ECS Chemical Vapor Deposition proceedings, 87-8,204, 1987

2. K. Benson, W. Lin, and P. Langer, "Silicon Preparation" - chapter in "Concise Encyclopedia of Electronic and Optoelectronic Materials," Pergamon Press

3. A.S. Grove, A. Roder, and C.T. Sah, "Impurity Distribution in Epitaxial Growth," J. Appl. Phys.,36,802 (1965).

4. Werner Juengling "BICEPS 5.0 User's Guide," AT&T Bell Laboratories Internal Memorandum, June 28, 1988.

5. Stephen E. Hansen, "SUPREM-III User's Manual, version 8520," Stanford University, May 7, 1985

6. Charles P. Ho and Stephen E. Hansen, "SUPREM III - A Program for Integrated Circuit Process Modeling and Simulation," Stanford University, Technical Report No. SEL 83-001, July 1983

7. Richard B. Fair, "Concentration Profiles of Diffused Dopants in Silicon," Chapter 7 of "Impurity Doping," F.F.Y. Wang, editor, North Holland Publishing Co., 1981

8. S.M. Sze, "Physics of Semiconductor Devices, 2nd Edition" John Wiley and Sons, Inc., 1981

9. F.J. Morin and J.P. Maita, "Electrical Properties of Silicon Containing Arsenic and Boron," Physical Review, Volume 96, Number 1, October 1, 1954

10. S.M.Sze, editor "VLSI Technology," McGraw-Hill, 1983

11. A.S. Grove, "Physics and Technology of Semiconductor Devices," Wiley 1967

12. ASTM F723, "ASTM Book of Standards," Vol 10.05 (II), 1988

13. J.A. McHugh, "Secondary Ion Mass Spectrometery," in A.W. Czanderna, Ed., "Methods of Surface Analysis", Elsevier, New York, 1975.

14. F.A. Stevie, P.M. Kahora, D.S. Simons, and P. Chi, "Secondary ion yield changes in Si and GaAs due to topography changes during O_2^+ or Cs^+ ion bombardment," J. Vac. Sci. Technol., A 6(1), 76 (1988)

15. D.A. Antoniadis, A.G. Gonzalez, and R.W. Dutton, "Boron in Near-Intrinsic < 100> and < 111> Silicon under Inert and Oxidizing Ambients - Diffusion and Segregation," J. Electrochem. Soc. 125, 813 (1978)

16. W.E. Beadle, J.C.C. Tsai, and R.D. Plummer editors, "Quick Reference Manual for Silicon Integrated Circuit Technology," John Wiley & Sons, Inc. 1985

17. W.R. Runyan, "Silicon Semiconductor Technology," McGraw Hill Book Co., 1965

APPENDIX A

```
title Run 1 1150 C Simulation   file=birun1
subs  elem=boron  conc=1.1e19  ornt=100 xdelta=0.01  xthick=3.0  oxide=0
*
comm  Ramp up from 850 to 1150 C
drive  temp=850  ambi=inert time=4.3 trte=70
*
comm  Stabilize and H2 bake
drive   temp=1150  time=10.7  ambi=inert
*
print kind=1
*
comm   Epitaxy  1.0 um/m  1150 C
epit   temp=1150 grte=1.0 time=10.0 elem=boron conc=1.6e15
*
comm   Post epi purge
drive   temp=1150  time=2  ambi=inert
*
comm   Ramp down to 850
drive   temp=1150  time=3  trte=-90  ambi=inert
*
print kind=1
*
end
```

BICEPS input for 1150° C run

```
TITLE       RUN 1 1150 C SIMULATION
$           FILE SUP1
$
INITIALIZE  SILICON  <100>  BORON  CONC=1.1E19 THICK=3.0  DX=0.02
$
COMMENT     RAMP UP FROM 850 TO 1150 C
DIFFUSION   TEMPERAT=850  TIME=4.3  NITROGEN  T.RATE=70
$
COMMENT     STABILIZE AND H2 BAKE
DIFFUSION   TEMPERAT=1150  TIME=10.7  NITROGEN
$
PRINT       MATERIAL SILICON IMPURITY BORON  FILE=n.sup1s
PRINT       BORON CHEMICAL CONCENTR FILE=a.sup1s COL=25 XMAX=12
$
COMMENT     EPITAXY  1.0 UM/M  1150 C
EPITAXY     BORON  TEMP=1150 TIME=10.0 GROWTH.R=1.0  CONC=1.6E15
$
COMMENT     POST EPI PURGE
DIFFUSION   TEMPERAT=1150  TIME=2  NITROGEN
$
COMMENT     RAMP DOWN TO 850
DIFFUSION   TEMPERAT=1150  TIME=3  T.RATE=-90  NITROGEN
$
PRINT       MATERIAL SILICON IMPURITY BORON  FILE=n.sup1
PRINT       MATERIAL BORON CHEMICAL CONCENTR FILE=a.sup1 COL=25 XMAX=12
$
STOP
```

SUPREM input for 1150° C run

VITA

Linda D. Snyder was born in Allentown, Pennsylvania on May 29, 1959 to Timothy G. and Patricia A. Snyder. She graduated from Dieruff High School, also in Allentown, with high honors, in June 1977. She did her undergraduate studies at Lehigh University and graduated magna cum laude with the degree of Bachelor of Science in Engineering Physics with a minor in Computer Science in May 1981. She joined Bell Telephone Laboratories in June 1981, starting as a Senior Technical Associate in the Silicon Processing Technology Laboratory.

At AT&T Bell Laboratories, she is presently a Member of the Technical Staff in the VLSI Technology Laboratory, working on the DDL cleanroom Computer Integrated Manufacturing (CIM) project, as a system manager/administrator and user interface.